

Variational integrators for the dynamics of thermo-elastic solids with finite speed thermal waves

Pablo Mata

Centro de Investigación en Ecosistemas de la Patagonia (CIEP),
Conicyt Regional/CIEP R10C1003, Universidad Austral de Chile,
Ignacio Serrano 509, Coyhaique, Chile.

Adrián J. Lew

Department of Mechanical Engineering, Stanford University,
Stanford, CA 94305-4040, USA
email:lewa@stanford.edu

January, 2014

Abstract

This paper formulates variational integrators for finite element discretizations of deformable bodies with heat conduction in the form of finite speed thermal waves. The cornerstone of the construction consists in taking advantage of the fact that the Green-Naghdi theory of type II for thermo-elastic solids has a Hamiltonian structure. Thus, standard techniques to construct variational integrators can be applied to finite element discretizations of the problem. The resulting discrete-in-time trajectories are then consistent with the laws of thermodynamics for these systems: for an isolated system, they exactly conserve the total entropy, and nearly exactly conserve the total energy over exponentially long periods of time. Moreover, linear and angular momenta are also exactly conserved whenever the exact system does. For definiteness, we construct an explicit second-order accurate algorithm for affine tetrahedral elements in two and three-dimensions, and demonstrate its performance with numerical examples.

Contents

1	Introduction	2
2	Continuum problem	4
2.1	Kinematics and constitutive relations	5
2.2	Lagrangian formulation	6
2.3	Conserved quantities	7
2.4	Examples	8
3	Discretization	10
3.1	Discretization in space	10
3.2	Discretization in time: variational integrators	12

4	Explicit algorithms	14
4.1	Gauss-Lobatto quadrature rule	14
4.2	First order with Δt	15
4.3	Second order with Δt — Autonomous case	16
4.4	Second order with Δt — Non-autonomous case	17
4.5	Explicit second-order algorithm $\hat{\mathbf{F}}_{h,\Delta t}^{10}$	17
4.6	A note on the use of a nodal quadrature	19
4.7	Conservation properties of the algorithms	19
4.8	Stability	20
5	Numerical examples	21
5.1	Convergence Properties of the Algorithm	21
5.2	Dynamics of a thermo-elastic three-dimensional body	22
6	Conclusions	25
A	Explicit expressions of derivatives of \mathbf{L}_h	26

1 Introduction

The classical treatment to describe heat conduction in solids adopts Fourier's law to describe the heat flux (e.g., [2, 3, 4]). In the context of thermo-elastic materials, this assumption leads to the transmission of thermal disturbances with infinite speed [1, 5]. Notwithstanding, this model has been found to be very useful in many engineering applications. On the other hand, since several decades ago (e.g. [6]) it has been recognized that heat transport with finite speed thermal waves may be useful in modeling some materials at low temperatures. This phenomenon is frequently mentioned in the literature as *second sound*, to differentiate it from the *first sound* in solids, which is related to the propagation of mechanical waves. Other contexts in which such theories could be useful are referred to in [7, 8, 9, 10].

A number of theories have been proposed to model heat transfer with finite speed thermal waves, e.g., [1, 11]. Among them, some incorporate a regularization of the heat flux to include a relaxation time controlling the velocity of propagation of heat perturbations [12, 13], see [14] for a thorough discussion. A variational theory for heat conduction in rigid solids with finite wave speed based on a non-autonomous Hamiltonian was considered in [15, 24, 16]. This approach recovers the classical Fourier case in the limit in which a relaxation parameter approaches zero. An attempt to extend these ideas to general problems of non-conservative type is described in [17], and a survey of such models can be found in [18]. Alternative variational principles are also available [19, 20, 21, 22]. More recently, a general variational framework for non-reversible processes was presented by Mielke and Ortiz [23].

One of the most well-known formulations for heat-conducting thermo-elasticity has been proposed by Green and Naghdi in a series of papers [25, 26, 27, 28, 29]. There, the authors take advantage of the concept of thermal displacements (see, e.g., [30, 31, 32] for a discussion) to construct three types theories: (i) the first one (type I) corresponds to the classical thermo-elasticity with heat conduction of Fourier type, (ii) the second (type II) corresponds to a theory able to predict the existence of undamped thermal waves traveling at finite speed, and finally, (iii) the third (type III) results from combining the first two types, see [33] for a recent discussion.

The Green and Naghdi theory of type II (G-N-II theory in what follows) is particularly interesting due to the fact that: (i) It is well suited for simulating second sounds in

thermo-elastic solids [5, 34], and (ii) the resulting evolution equations possess an autonomous Hamiltonian structure [31]. This structure is unveiled after taking into account that the thermal displacement, temperature and entropy fields work in a complete analogy to how the (mechanical) displacement, velocity and momentum fields do in an elastic problem. In this case, the heat flux depends on the gradient of the thermal displacements, and therefore, heat conduction depends on the “thermal strains.” We will outline the essential structure of this theory in the following sections.

A number of results are available for some versions of G-N-II. The existence, uniqueness and the qualitative behavior of solutions for the linear theory of thermoelasticity without energy dissipation in the general anisotropic case has been studied by Quintanilla [35]. Additionally, suitable conditions under which the problem is well-posed are determined. In [36] the same author proposes a model extending the theory to the case of non-simple elastic materials, by allowing the Helmholtz free energy density of the material to depend on the second derivatives of the displacements. In [37] a discussion about G-N-III theory is presented. Chandrasekharaiah [38] studies uniqueness of solutions for initial, mixed boundary value problems considering homogeneous and isotropic materials. In [39] the one-dimensional propagation of a Heaviside-shaped thermal pulse in a half-space is investigated analytically, and in [40] the G-N theories are treated in the context of the material force method.

The design and construction of numerical methods for thermo-mechanical systems has a long history, see e.g. [41, 42, 43, 44, 45] to name only a few. Outstanding among them are so called fractional-step-methods, originally presented by Armero and Simo [41], which are based on the splitting of the evolution equations in an adiabatic phase followed by a conductive phase. The resulting algorithms may be made unconditionally stable, but they are only first-order accurate and, in general, implicit. A goal in this area is to design *thermodynamically consistent* methods [46, 47], namely, methods whose trajectories satisfy the first and second law of thermodynamics. This means that the discrete trajectories should satisfy that, for an isolated system, the energy of the system is conserved, and the entropy of the system does not decrease in time. A step in this direction is given by the extension of energy-momentum methods [49, 48, 50, 51] to the thermo-elastic case, see e.g., [52, 53, 54, 55] among others. A different approach to designing thermodynamically consistent methods is followed by Romero [47, 56]. Therein, the author creates structure-preserving discretizations of the so-called GENERIC formalism [57], which conserve the invariants of the system even in the case of heat conduction of Fourier type.

There is a shorter list of numerical methods for simulating second sound. Bargmann and Steinmann [34, 58, 59] build a finite-element-based discretization in space and time. Moreover, they use the resulting method to simulate the propagation of second sound at cryogenic temperatures. An incremental formulation based in part on an adequate discretization of the Euler-Lagrange (EL) equations is presented in [60] by the same authors.

The construction of integrators for which the trajectories preserve invariants of the original system is the realm of structured or geometric integration, see e.g. [61, 62, 63]. Variational integrators (VI) provide a way to design structure-preserving time integrators for problems whose dynamics is generated by a Hamiltonian. The basic idea behind these methods is to obtain the algorithm from discrete analog to Hamilton’s variational principle. In this way, the computed discrete trajectories are stationary points of a discrete action functional, the discrete action sum. As a result, the discrete trajectories approximate the exact trajectories of the system, and nearly exactly preserve the exact energy of the system for long times [62, Ch. 9]. Moreover, if the discrete action sum is designed to respect symmetries of the original action functional, then by virtue of a discrete version of Noether’s theorem, the discrete trajectories conserve the momenta conjugate to each one of these symmetries, see e.g. [64]. Finally, the resulting algorithms are symplectic by design. Nowadays it is

possible to find a vast literature on VIs. Most of the basic theory and analytical results may be reviewed in [65, 66, 67, 64, 68, 69, 70].

These methods have been successfully applied in numerous fields, such as to the construction of asynchronous integration methods in solid mechanics [64, 68], to problems with constraints [69, 71], to problems with contact [72, 73, 74, 75], with oscillatory solutions [76], to Langevin and stochastic differential equations [77, 78], to problems where the evolution takes place over a nonlinear manifold [79, 80], and to incompressible fluids [81], to name some of the most relevant ones.

In an earlier work [46] we constructed VI for finite dimensional thermo-elastic mechanical systems without heat conduction. To construct such integrators we exploited the Hamiltonian structure of such systems once the thermal displacements are introduced. The resulting algorithms correspond to a family of symplectic, entropy- and momentum-conserving, implicit and explicit Runge-Kutta methods. The formulation of an explicit second-order method was particularly challenging in this case, since the dependence of the Lagrangian on the thermal velocities (temperatures) was other than quadratic. It turns out then that the standard discrete Lagrangian that leads to the central differences or Newmark’s second-order explicit algorithm renders an implicit algorithm for these systems. Instead, we constructed a second-order explicit algorithm by composing a first-order method with its adjoint.

In this paper, we extend those ideas to the case of a thermo-elastic continuum according to G-N-II theory [25]. We begin in §2 by reviewing the Lagrangian formulation of the G-N-II theory, including a discussion about symmetries and conserved quantities. The Euler-Lagrange equations of this system are the balance of mechanical and thermal momenta. The latter is none other than the evolution of the entropy density. In particular, the conservation of the total entropy for isolated systems is a consequence of the invariance of the Lagrangian density with respect to rigid translations of the thermal displacements. This conservation property is added to the classical conservation of energy and momenta appearing in (isolated) elastic systems.

We construct a general class of time-integrators in §3. To this end, we first construct a finite-dimensional mechanical system by introducing a finite element discretization in space and a general class of quadrature rules. In particular, we only consider simplicial meshes of continuous P_1 finite elements. The construction of variational integrators then follows in a standard way. The resulting integrators are generally implicit. We then construct explicit integrators in §4 by: (a) selecting two first-order time integrators from the general class in §3, the so-called *Euler-A* and *Euler-B* methods, and (b) selecting a quadrature rule with quadrature points at the nodes of the mesh (Gauss-Lobatto rule). Second-order accuracy follows by composing these two methods, since they are mutually adjoint [69]. This leads to two different but related second-order methods. A similar construction does not lead to explicit higher-order methods, because of the order of the quadrature rule, so these are not addressed here. The numerical performance of the algorithms is examined in §5 through several examples, and we finish the paper with some conclusions in §6.

2 Continuum problem

In this section a Lagrangian formulation for the G-N-II of thermoelasticity [25] is presented following the ideas described in [32, 30, 31, 82]. The basic ingredient of this construction is the inclusion of a *thermal displacement field* over the continuum, in addition to the mechanical displacement field, and a free-energy that depends on the “thermal strains.” As a consequence, the balance equation for the entropy of the system permits the propagation of thermal waves of finite speed, due to the appearance of entropy fluxes (or “thermal stresses”)

that depend on the gradient of the thermal displacements.

2.1 Kinematics and constitutive relations

Consider a body with reference configuration $\Omega \subset \mathbb{R}^d$, $d \in \{1, 2, 3\}$, where Ω is a bounded open set with piecewise smooth boundary $\partial\Omega$ ¹. The deformation of the body is described by a motion $\varphi(\mathbf{X}, t)$, which returns the position in \mathbb{R}^d at time t of the continuum particle at $\mathbf{X} \in \Omega$. Similarly, consider the thermal displacement field $\Phi(\mathbf{X}, t)$, a real-valued function which in the context of this theory is an additional kinematic variable [32, 31, 82]. A thermo-elastic deformation of the body is described then as (φ, Φ) . The spatial gradient of a thermo-elastic deformation are the deformation gradient $\mathbf{F} = \nabla\varphi$ and the thermal displacement gradient $\boldsymbol{\beta} = \nabla\Phi$. The temporal derivatives include the velocity field $\mathbf{v} = \dot{\varphi}$ and the *empirical temperature* field $\theta = \dot{\Phi}$, which is the distinguishing feature of the thermal displacements.

Following Green-Naghdi's theory of type II for non-classical thermo-elasticity [32, 26, 25], we assume that the Helmholtz free energy density per unit of mass is a smooth real-valued, material-frame indifferent function

$$A(\mathbf{F}, \boldsymbol{\beta}, \theta; \mathbf{X}). \quad (1)$$

Its distinctive feature is that it depends on $\boldsymbol{\beta}$, the gradient of the thermal displacements. The function A serves then as the thermodynamic potential for the first Piola-Kirchhoff stress tensor \mathbf{P} , the entropy density per unit mass η , and the entropy flux vector (per unit area in the reference configuration) \mathbf{h} , as follows

$$\mathbf{P} = \rho_0 \frac{\partial A}{\partial \mathbf{F}}, \quad \eta = -\frac{\partial A}{\partial \theta}, \quad \mathbf{h} = -\rho_0 \frac{\partial A}{\partial \boldsymbol{\beta}}, \quad (2)$$

where $\rho_0(\mathbf{X})$ is the mass density per unit volume in the reference configuration. If, for example, A is strictly convex with respect to θ , it is possible to invert (2)₂ for each value of \mathbf{F} and $\boldsymbol{\beta}$ to compute the temperature as

$$\theta = \hat{\theta}(\mathbf{F}, \boldsymbol{\beta}, \eta; \mathbf{X}). \quad (3)$$

The heat flux vector \mathbf{q} (per unit area in the reference configuration) follows from the constitutive relation (2)₃ as

$$\mathbf{q} = \theta \mathbf{h}. \quad (4)$$

Finally, for future reference we also introduce the internal energy density per unit mass as

$$U(\mathbf{F}, \boldsymbol{\beta}, \eta; \mathbf{X}) = \eta \hat{\theta}(\mathbf{F}, \boldsymbol{\beta}, \eta; \mathbf{X}) + A(\mathbf{F}, \boldsymbol{\beta}, \hat{\theta}(\mathbf{F}, \boldsymbol{\beta}, \eta; \mathbf{X}); \mathbf{X}). \quad (5)$$

In the following we shall assume that the material is spatially homogeneous, namely, that A and hence U do not depend explicitly on \mathbf{X} . We also assume that A is a strictly convex function of θ for all possible values $(\mathbf{F}, \boldsymbol{\beta})$. Additionally, to obtain an explicit algorithm, we assume that $\partial^2 A / \partial \boldsymbol{\beta} \partial \theta = 0$, i.e., there is no dependence of η on $\boldsymbol{\beta}$ and of \mathbf{h} on θ . This assumption is satisfied by standard models in the literature for this type of heat conduction.

¹For simplicity, polyhedral, so that it can be exactly meshed, although curved domains can be handled in a "natural" way.

2.2 Lagrangian formulation

A unique feature of this theory is that the local form of the balance equations for the stresses and the entropy density are the Euler-Lagrange equations of Hamilton's principle with a suitable action functional. To this end, we define the appropriate Lagrangian as

$$\mathbf{L}(\boldsymbol{\varphi}, \Phi, \mathbf{v}, \theta) := \mathbf{K}(\mathbf{v}) - \mathbf{W}(\boldsymbol{\varphi}, \Phi, \theta) - \mathbf{E}(\boldsymbol{\varphi}, \Phi), \quad (6)$$

where $\mathbf{K}(\mathbf{v})$ corresponds to the kinetic energy and it is given by

$$\mathbf{K}(\mathbf{v}) = \frac{1}{2} \int_{\Omega} \rho_0 \mathbf{v} \cdot \mathbf{v} \, dV, \quad (7)$$

the function $\mathbf{W}(\boldsymbol{\varphi}, \Phi, \theta)$ is the total Helmholtz free energy of the body,

$$\mathbf{W}(\boldsymbol{\varphi}, \Phi, \theta) = \int_{\Omega} \rho_0 \mathbf{A}(\nabla \boldsymbol{\varphi}, \nabla \Phi, \theta) \, dV, \quad (8)$$

and the remaining term $\mathbf{E}(\boldsymbol{\varphi}, \Phi)$ stems from the action of external agents acting on the system. For this term we assume the existence of a conservative body force per unit mass $\mathbf{B} = -dV_B(\boldsymbol{\varphi})/d\boldsymbol{\varphi}$, for a potential function V_B . Additionally, we consider an entropy source per unit mass $\mathbf{Q}: \Omega \rightarrow \mathbb{R}$, and a traction field $\mathbf{T}: \Gamma_t \subset \partial\Omega \rightarrow \mathbb{R}^d$ and an entropy flux into the body $\bar{\mathbf{h}}: \Gamma_h \subset \partial\Omega \rightarrow \mathbb{R}$ (both per unit area in the reference configuration). Under these conditions, we have

$$\mathbf{E}(\boldsymbol{\varphi}, \Phi) = \int_{\Omega} \rho_0 (V_B(\boldsymbol{\varphi}) - \mathbf{Q} \Phi) \, dV - \int_{\Gamma_t} \mathbf{T} \cdot \boldsymbol{\varphi} \, dS - \int_{\Gamma_h} \bar{\mathbf{h}} \Phi \, dS. \quad (9)$$

To formulate Hamilton's principle, consider the set \mathcal{C} of smooth enough motions $(\boldsymbol{\varphi}, \Phi)$ during the time interval $[0, T]$ between two prescribed configurations $(\boldsymbol{\varphi}, \Phi)|_{t=0} = (\boldsymbol{\varphi}_0, \Phi_0)$ and $(\boldsymbol{\varphi}, \Phi)|_{t=T} = (\boldsymbol{\varphi}_T, \Phi_T)$. Motions in \mathcal{C} are assumed to satisfy boundary conditions on $\Gamma_{\varphi} = \partial\Omega \setminus \Gamma_t$ and $\Gamma_{\Phi} = \partial\Omega \setminus \Gamma_h$ according to

$$\boldsymbol{\varphi}(\cdot, t)|_{\Gamma_{\varphi}} = \bar{\boldsymbol{\varphi}}(\cdot, t) \quad \text{and} \quad \Phi(\cdot, t)|_{\Gamma_{\Phi}} = \bar{\Phi}(\cdot, t) \quad (10)$$

for all $t \in (0, T)$, where $\bar{\boldsymbol{\varphi}}: \Gamma_{\varphi} \times (0, T) \rightarrow \mathbb{R}^d$ and $\bar{\Phi}: \Gamma_{\Phi} \times (0, T) \rightarrow \mathbb{R}$ are prescribed. Then, the action functional $\mathbf{S}: \mathcal{C} \rightarrow \mathbb{R}$ is given by

$$\mathbf{S}(\boldsymbol{\varphi}, \Phi) = \int_0^T \mathbf{L}(\boldsymbol{\varphi}, \Phi, \dot{\boldsymbol{\varphi}}, \dot{\Phi}) \, dt. \quad (11)$$

Hamilton's principle states that the trajectory followed by the system corresponds to a stationary point of the action in \mathcal{C} . In other words, the problem of studying the motion of a thermo-elastic system consist in finding $(\boldsymbol{\varphi}, \Phi) \in \mathcal{C}$ such that

$$\delta \mathbf{S} = 0,$$

for all admissible variations $(\delta \boldsymbol{\varphi}, \delta \Phi)$ (in \mathcal{TC}).

Therefore, taking the first variation of (11), integrating by parts in time and applying the divergence theorem in the space variables yields

$$\begin{aligned} \delta \mathbf{S} &= \int_0^T \int_{\Omega} \left[(\nabla \cdot \mathbf{P} + \rho_0 \mathbf{B} - \rho_0 \ddot{\boldsymbol{\varphi}}) \cdot \delta \boldsymbol{\varphi} + (\rho_0 \mathbf{Q} - \nabla \cdot \mathbf{h} - \rho_0 \dot{\eta}) \delta \Phi \right] dV \, dt + \\ &+ \int_0^T \left[\int_{\Gamma_t} (\mathbf{T} - \mathbf{P} \mathbf{n}) \cdot \delta \boldsymbol{\varphi} \, dS + \int_{\Gamma_h} (\bar{\mathbf{h}} + \mathbf{h} \cdot \mathbf{n}) \delta \Phi \, dS \right] dt = 0, \end{aligned} \quad (12)$$

where \mathbf{n} is the outward normal to $\partial\Omega$. Then, the following system of Euler-Lagrange equations are obtained

$$\rho_0 \ddot{\boldsymbol{\varphi}} = \nabla \cdot \mathbf{P} + \rho_0 \mathbf{B}, \quad \text{in } \Omega \times [0, T], \quad (13a)$$

$$\rho_0 \dot{\eta} = \rho_0 Q - \nabla \cdot \mathbf{h}, \quad \text{in } \Omega \times [0, T], \quad (13b)$$

$$\mathbf{P}\mathbf{n} = \mathbf{T}, \quad \text{on } \Gamma_t \times [0, T], \quad (13c)$$

$$-\mathbf{h} \cdot \mathbf{n} = \bar{h}, \quad \text{on } \Gamma_h \times [0, T]. \quad (13d)$$

An initial value problem is obtained by complementing these equations with the boundary conditions (10) and initial conditions

$$(\boldsymbol{\varphi}, \Phi)|_{t=0} = (\boldsymbol{\varphi}_0, \Phi_0) \quad \text{and} \quad (\dot{\boldsymbol{\varphi}}, \theta)|_{t=0} = (\mathbf{v}_0, \theta_0) \quad \text{in } \Omega. \quad (13e)$$

Some remarks are now pertinent:

- (i) The local balance of linear momentum is stated in (13a). Additionally, the entropy balance equation (13b) appears as a consequence of the variational principle. By expanding its left hand side the following mechanically-coupled heat equation is obtained

$$\frac{\partial \eta}{\partial \mathbf{F}} : \dot{\mathbf{F}} + \frac{\partial \eta}{\partial \theta} \dot{\theta} = Q - \frac{1}{\rho_0} \nabla \cdot \mathbf{h},$$

in which time derivatives of only $(\boldsymbol{\varphi}, \Phi)$ appear.

- (ii) These equations are formally identical to those for thermo-elasticity based on Fourier's law. The key difference lies in that here \mathbf{h} depends on $\nabla \Phi$, while in the classical case \mathbf{h} depends on $\nabla \Phi$.
- (iii) From Clausius-Duhem inequality the internal rate of entropy production should satisfy

$$\zeta = \rho_0(\dot{\eta} - Q) + \nabla \cdot \mathbf{h} \geq 0. \quad (14)$$

From (13b), it follows that $\zeta = 0$ even in the presence of heat conduction. This why this theory is referred to as *thermo-elasticity without energy dissipation* [25, 1].

2.3 Conserved quantities

According to Noether's theorem (see, e.g., [3, 70]) if the Lagrangian of the system remains invariant under the action of a group on the configuration space, there exists a corresponding quantity which is conserved by the dynamics. In this section, conserved quantities are reviewed for the G-N-II theory of thermo-elasticity. For simplicity, in this section we assume that $\Gamma_{\boldsymbol{\varphi}} = \Gamma_{\Phi} = \emptyset$.

Energy conservation The Lagrangian functional (6) is autonomous and therefore invariant under translations in time (some times called horizontal translations, see e.g. [83, 69] and references therein). It is well known that for such systems the associated conserved quantity is the value of the Hamiltonian function, which is that of the total energy. An alternative way to see this is by direct computation of the time derivative of the Hamiltonian function, verifying that it is exactly equal to zero if the Euler-Lagrange equations (13a)–(13d) are satisfied.

Linear and angular momentum conservation If $\mathbf{B} = 0$, $\mathbf{Q} = 0$, $\mathbf{T} = 0$ and $\bar{\mathbf{h}} = 0$, the Lagrangian (6) is invariant under the action of rigid body translations and rotations in space. A well-known consequence is that the linear and angular momentum of the system are conserved in time.

Conservation of the total entropy Conservation of energy and linear and angular momentum are features shared with classical elastodynamics. The hallmark feature of this theory is that, in the absence of entropy sources ($\mathbf{Q} = 0$ and $\bar{\mathbf{h}} = 0$), the entropy of the system does not increase even in the presence of heat conduction.

A simple way to see this is to integrate (13b) over Ω and apply the divergence theorem to obtain the time derivative of the total entropy Ξ , namely,

$$\dot{\Xi} := \int_{\Omega} \rho_0 \dot{\eta} dV = - \int_{\partial\Omega} \mathbf{h} \cdot \mathbf{n} dS = 0. \quad (15)$$

An alternative perspective on this conservation law is as a symmetry of the Lagrangian. More precisely, the total entropy appears as the conserved quantity associated to the invariance of the Lagrangian under the continuous transformation of the thermal displacements $\Phi_{\epsilon} \equiv \Phi + \epsilon \zeta$ for and $\zeta \in \mathbb{R}$ and any $\epsilon \in \mathbb{R}$. This symmetry is stated as

$$\mathbf{L}_{\epsilon} \equiv \mathbf{L}(\boldsymbol{\varphi}, \dot{\boldsymbol{\varphi}}, \nabla \Phi_{\epsilon}, \dot{\Phi}_{\epsilon}) = \mathbf{L}(\boldsymbol{\varphi}, \dot{\boldsymbol{\varphi}}, \nabla \Phi_0, \dot{\Phi}_0) = \mathbf{L}_0, \quad (16)$$

after noting that $\nabla \Phi_{\epsilon} = \nabla \Phi$ and $\dot{\Phi}_{\epsilon} = \dot{\Phi}$. The conserved quantity associated to this symmetry can be unveiled by computing

$$0 = \frac{d}{d\epsilon} \mathbf{L}_{\epsilon} \Big|_{\epsilon=0} = \int_{\Omega} \left(\rho_0 \eta \frac{d}{dt} \zeta + \nabla \cdot \mathbf{h} \zeta \right) dV = \int_{\Omega} \left(\rho_0 \eta \frac{d}{dt} \zeta - \rho_0 \dot{\eta} \zeta \right) dV = \zeta \frac{d}{dt} \int_{\Omega} \rho_0 \eta dV, \quad (17)$$

where we have used (13b) and (13d). The fact that $\dot{\Xi} = 0$ follows by setting $\zeta \neq 0$.

If the body is in thermal contact with the surrounding environment, we have that the entropy source \mathbf{Q} and entropy flux $\bar{\mathbf{h}}$ modify the above equation according to

$$\dot{\Xi} = \int_{\Omega} \mathbf{Q} dV + \int_{\Gamma_h} \bar{\mathbf{h}} dS, \quad (18)$$

which clearly shows that the time evolution of the total entropy in the system depends on the signs and magnitudes of the external sources and fluxes.

2.4 Examples

In this section we show two examples of constitutive relations for G-N-II thermo-elastic materials.

Example of linear thermo-elasticity A possible form for the Helmholtz free energy density per unit mass for the case of infinitesimal deformations is given by

$$A(\mathbf{F}, \boldsymbol{\beta}, \theta) = \frac{1}{2\rho_0} \mathbf{e} : \mathbf{C} : \mathbf{e} - \frac{c}{2\theta_0} (\theta - \theta_0)^2 - \gamma (\theta - \theta_0) \mathbf{e} : \mathbf{I} - (\theta - \theta_0) \eta_0 + \frac{\kappa}{2\rho_0} \boldsymbol{\beta} \cdot \boldsymbol{\beta},$$

where the operator $:$ indicates double contraction of indices, $\mathbf{e} = \frac{1}{2}(\mathbf{F} + \mathbf{F}^t - 2\mathbf{I})$ is the small strain tensor, \mathbf{C} are the linear elastic moduli (assumed to have major and minor symmetries), c is a specific heat, γ is a thermo-mechanical coupling parameter, κ is a non-classical thermal

conductivity constant, and θ_0 and η_0 are the reference temperature and reference entropy, respectively.

Therefore, the entropy flux vector, the internal entropy density, the temperature, and the Cauchy stress tensor (which coincides with \mathbf{P} in the infinitesimal deformations case) are given by

$$\mathbf{h} = -\kappa\boldsymbol{\beta}, \quad (19a)$$

$$\eta = \frac{c}{\theta_0}(\theta - \theta_0) + \gamma\mathbf{e} : \mathbf{I} + \eta_0, \quad (19b)$$

$$\theta = \theta_0 \left(1 + \frac{\eta - \eta_0 - \gamma\mathbf{e} : \mathbf{I}}{c} \right), \quad (19c)$$

$$\boldsymbol{\sigma} = \mathbf{C} : \mathbf{e} - \rho_0\gamma(\theta - \theta_0)\mathbf{I}. \quad (19d)$$

The corresponding balance equations are given by

$$\begin{aligned} \nabla \cdot (\mathbf{C} : \mathbf{e}) - \rho_0\gamma\nabla\theta &= \rho_0(\ddot{\boldsymbol{\varphi}} - \mathbf{B}), \\ \frac{c}{\theta_0}\dot{\theta} + \gamma\dot{\mathbf{e}} : \mathbf{I} &= \mathbf{Q} + \frac{\kappa}{\rho_0}\nabla \cdot \boldsymbol{\beta}. \end{aligned}$$

One-dimensional harmonic solutions: It is interesting to find one-dimensional harmonic solutions of these equations, since they reveal coupled thermo-mechanical waveforms that propagate without distortion. Assuming that the material is isotropic, that $\Phi(\mathbf{X}, t) \equiv \Phi(X, t)$, $\boldsymbol{\varphi}(\mathbf{X}, t) = \mathbf{X} + u(X, t)\mathbf{e}_X$, where \mathbf{e}_X is the unit vector in the X -direction, and in the absence of external loading ($\mathbf{B} = 0$, $\mathbf{Q} = 0$), the above equations reduce to

$$\ddot{u} = \left(\frac{E}{\rho_0} \right) u_{,XX} - \gamma\dot{\Phi}_{,X}, \quad (20a)$$

$$\ddot{\Phi} = \left(\frac{\kappa\theta_0}{c\rho_0} \right) \Phi_{,XX} - \left(\frac{\gamma\theta_0}{c} \right) \dot{u}_{,X}. \quad (20b)$$

Here E is the effective stiffness of the material in this case. We consider traveling wave solutions of the type $u(X, t) = \Re[A_\varphi \exp[i(KX + \omega t)]]$ and $\Phi(X, t) = \Re[A_\Phi \exp[i(KX + \omega t)]]$, which after replacing in the above equations yield the following four dispersion relations

$$\omega_{\pm\pm} = \pm K \sqrt{\frac{\theta_0(\rho_0\gamma^2 + \kappa) + cE \pm \sqrt{\rho_0^2\theta_0^2\gamma^4 + 2\rho_0\theta_0\gamma^2(cE + \kappa\theta_0) + (cE - \kappa\theta_0)^2}}{2c\rho_0}}. \quad (21)$$

A special case of this dispersion relation is obtained by setting $\gamma = 0$ (no thermo-mechanical coupling), from where we recover the dispersion relations for the thermal and mechanical waves [34, 58]

$$\frac{d\omega}{dK} = \pm \sqrt{\frac{E}{\rho_0}} \quad \text{and} \quad \frac{d\omega}{dK} = \pm \sqrt{\frac{\kappa\theta_0}{c\rho_0}},$$

respectively. Moreover, if we consider the case $\kappa = 0$ and $\gamma > 0$, we obtain the dispersion relation corresponding to an adiabatic thermo-mechanical wave, namely,

$$\frac{d\omega}{dK} = \pm \sqrt{\frac{\rho_0\theta_0\gamma^2 + cE}{c\rho_0}}.$$

Example in nonlinear thermo-elasticity One form for the Helmholtz free energy density per unit mass in the large deformations case is given by

$$\begin{aligned} A(\mathbf{F}, \boldsymbol{\beta}, \theta) = & \frac{\mu}{2\rho_0} \mathbf{F} : \mathbf{F} + \frac{\lambda}{2\rho_0} \ln^2 J - \frac{\mu}{\rho_0} \ln J - \gamma(\theta - \theta_0) \ln J \\ & + c \left(\theta - \theta_0 - \theta \ln \left(\frac{\theta}{\theta_0} \right) \right) - (\theta - \theta_0) \eta_0 + \frac{\kappa}{2\rho_0} \boldsymbol{\beta} \cdot \boldsymbol{\beta}, \end{aligned} \quad (22)$$

where γ , κ , ρ_0 and c are defined as in the previous example, $J = \det(\mathbf{F})$, and $\lambda, \mu > 0$ are elastic constants. It follows from here that

$$\mathbf{h} = -\kappa \boldsymbol{\beta}, \quad (23a)$$

$$\eta = c \ln \left(\frac{\theta}{\theta_0} \right) + \gamma \ln J + \eta_0, \quad (23b)$$

$$\theta = \theta_0 \exp \left[\frac{\eta - \eta_0 - \gamma \ln J}{c} \right], \quad (23c)$$

$$\mathbf{P} = \mu \mathbf{F} + (\lambda \ln J - \mu - \rho_0 \gamma (\theta - \theta_0)) \mathbf{F}^{-\top}. \quad (23d)$$

3 Discretization

We next construct new variational integrators to approximate the motions of bodies made of thermo-elastic material obeying the G-N-II theory of heat conduction. We accomplish this by following the same steps as in [68] for nonlinear elasticity. We first introduce a finite element discretization of the body in space and obtain semi-discrete equations of evolution in time for its degrees of freedom. Variational integrators in time are then constructed for the resulting finite dimensional system.

The variational integrators here constructed enjoy a number of important properties which will be described in detail in the following sections: (i) they are symplectic, (ii) they exactly conserve linear and angular momentum whenever they have to be conserved, (iii) they ensure the exact conservation of the total entropy for thermally isolated systems, and (iv) they display a bounded grow in the error of the computed energy which remains close to the exact value for exponentially long periods of time.

3.1 Discretization in space

Consider a triangulation \mathcal{T}_h of Ω with N nodes, where h is the maximum diameter of an element in \mathcal{T}_h , in which Γ_t and Γ_h are exactly meshed by the restriction of \mathcal{T}_h to $\partial\Omega$. We focus here on first- and second-order integration algorithms, so we consider a finite element space V_h of continuous functions that are affine over each element of the mesh. Discrete thermo-elastic deformations $(\boldsymbol{\varphi}_h(\cdot, t), \Phi_h(\cdot, t)) \in V_h^{d+1}$ can then be expressed as

$$(\boldsymbol{\varphi}_h(\mathbf{X}, t), \Phi_h(\mathbf{X}, t)) = \left(\sum_{a=1}^N N_a(\mathbf{X}) \boldsymbol{\varphi}_a(t), \sum_{a=1}^N N_a(\mathbf{X}) \Phi_a(t) \right), \quad (24)$$

where $\boldsymbol{\varphi}_a = (\varphi_a^1, \dots, \varphi_a^d)$ and Φ_a denote the value at node a of the motion and the thermal position, respectively, at any time. Correspondingly, $\{N_a\}_{a=1}^N$ is the set of dual basis functions in V_h to this choice of degrees of freedom for each scalar field, i.e., the standard “hat” functions over meshes of triangles or tetrahedra.

We next obtain the semi-discrete equations that describe the evolution in time of the degrees of freedom in the mesh. To this end, we approximate the values of (7), (8) and (9) by selecting quadrature rules, namely, we define functions $\mathbf{K}_h: V_h^d \rightarrow \mathbb{R}$, $\mathbf{W}_h: V_h^d \times V_h \times V_h \rightarrow \mathbb{R}$, and $\mathbf{E}_h: V_h^d \times V_h \rightarrow \mathbb{R}$ as

$$\mathbf{K}_h(\mathbf{v}_h) = \frac{\rho_0}{2} \sum_{i=1}^{N_q} w_i \mathbf{v}_h(\boldsymbol{\xi}_i) \cdot \mathbf{v}_h(\boldsymbol{\xi}_i), \quad (25a)$$

$$\mathbf{W}_h(\boldsymbol{\varphi}_h, \Phi_h, \theta_h) = \rho_0 \sum_{i=1}^{N_q} w_i \mathbf{A}(\nabla \boldsymbol{\varphi}_h(\boldsymbol{\xi}_i), \nabla \Phi_h(\boldsymbol{\xi}_i), \theta_h(\boldsymbol{\xi}_i)), \quad (25b)$$

$$\mathbf{E}_h(\boldsymbol{\varphi}_h, \Phi_h) = \sum_{i=1}^{N_q} w_i \rho_0 (V_B(\boldsymbol{\varphi}_h(\boldsymbol{\xi}_i)) - Q \Phi_h(\boldsymbol{\xi}_i)) - \sum_{j=1}^{N_t} w_j^t (\mathbf{T} \cdot \boldsymbol{\varphi})(\boldsymbol{\xi}_j^t) - \sum_{j=1}^{N_h} w_j^h (\bar{\mathbf{h}} \cdot \Phi)(\boldsymbol{\xi}_j^h)$$

where $\{w_i, \boldsymbol{\xi}_i\}_{i=1}^{N_q}$, $\{w_j^h, \boldsymbol{\xi}_j^h\}_{j=1}^{N_h}$ and $\{w_j^t, \boldsymbol{\xi}_j^t\}_{j=1}^{N_t}$ are quadrature points and weights over Ω , Γ_h and Γ_t , respectively. The Lagrangian for the semi-discrete system is

$$\mathbf{L}_h(\boldsymbol{\varphi}_h, \Phi_h, \mathbf{v}_h, \theta_h) = \mathbf{K}_h(\mathbf{v}_h) - \mathbf{W}_h(\boldsymbol{\varphi}_h, \Phi_h, \theta_h) - \mathbf{E}_h(\boldsymbol{\varphi}_h, \Phi_h). \quad (26)$$

The equations of motion for the semi-discrete system follow from the application of Hamilton's principle with this Lagrangian, as described next. Thermo-elastic deformations $(\boldsymbol{\varphi}_h, \Phi_h)$ of the semi-discrete system can be succinctly specified through the evolution of all nodal values $(\boldsymbol{\varphi}_a(\cdot), \Phi_a(\cdot))$, where unless otherwise specified, a runs from 1 to the number of nodes in the mesh N . Consider then the set \mathcal{C}_h of smooth enough motions $(\boldsymbol{\varphi}_a(\cdot), \Phi_a(\cdot))$ during the time interval $[0, T]$ between two prescribed configurations $(\boldsymbol{\varphi}_a(0), \Phi_a(0)) = (\boldsymbol{\varphi}_0(\mathbf{X}_a), \Phi_0(\mathbf{X}_a))$ and $(\boldsymbol{\varphi}_a(T), \Phi_a(T)) = (\boldsymbol{\varphi}_T(\mathbf{X}_a), \Phi_T(\mathbf{X}_a))$, which satisfy the boundary conditions

$$\begin{aligned} \boldsymbol{\varphi}_a(t) &= \bar{\boldsymbol{\varphi}}(\mathbf{X}_a, t), \quad \text{for all } \mathbf{X}_a \in \Gamma_\varphi \\ \Phi_a(t) &= \bar{\Phi}(\mathbf{X}_a, t), \quad \text{for all } \mathbf{X}_a \in \Gamma_\Phi, \end{aligned} \quad (27)$$

for all $t \in [0, T]$. Here $\mathbf{X}_a \in \bar{\Omega}$ denotes the position of node a . Trajectories of the system are the stationary points in \mathcal{C}_h of the action functional

$$S_h(\boldsymbol{\varphi}_a(\cdot), \Phi_a(\cdot)) = \int_0^T \mathbf{L}_h(\boldsymbol{\varphi}_h, \Phi_h, \dot{\boldsymbol{\varphi}}_h, \dot{\Phi}_h) dt. \quad (28)$$

The corresponding Euler-Lagrange equations are

$$\sum_{b=1}^N m_{ab} \ddot{\boldsymbol{\varphi}}_b = -\mathbf{S}_a + \mathbf{B}_a, \quad \mathbf{X}_a \notin \Gamma_\varphi \quad (29a)$$

$$\frac{d}{dt} \Upsilon_a(\boldsymbol{\varphi}_h, \Phi_h, \dot{\Phi}_h) = Q_a + H_a, \quad \mathbf{X}_a \notin \Gamma_\Phi \quad (29b)$$

for $a = 1, \dots, N$, where

$$m_{ab} = \rho_0 \sum_{i=1}^{N_q} w_i N_a(\boldsymbol{\xi}_i) N_b(\boldsymbol{\xi}_i) \quad (29c)$$

is the ab -component of the consistent mass matrix m , and

$$\mathbf{S}_a = \frac{\partial \mathbf{W}_h}{\partial \boldsymbol{\varphi}_a}, \quad \mathbf{B}_a = -\frac{\partial \mathbf{E}_h}{\partial \boldsymbol{\varphi}_a}, \quad Q_a = -\frac{\partial \mathbf{E}_h}{\partial \Phi_a}, \quad \Upsilon_a = -\frac{\partial \mathbf{W}_h}{\partial \theta_a}, \quad H_a = -\frac{\partial \mathbf{W}_h}{\partial \Phi_a}. \quad (29d)$$

All partial derivatives in (29) are computed by keeping all other nodal values constant. These equations have to be complemented with appropriate initial and boundary conditions.

The semi-discrete problem (29), obtained after introducing the finite element discretization in space, is a system of ordinary differential equations (ODEs) for $(\varphi_a(\cdot), \Phi_a(\cdot))$. Therefore, most of the standard techniques for solving ODEs numerically apply, including in this case structured or geometric integrators, e.g., [62]. Of course, a new semi-discrete problem is obtained for each mesh, but the L^2 -norm of $(\varphi - \varphi_h, \Phi - \Phi_h, \dot{\varphi} - \dot{\varphi}_h, \theta - \theta_h)$ is expected to be $\mathcal{O}(h^2)$ for smooth solutions. We show this with examples later on.

Hamiltonian perspective The transition to the Hamiltonian point of view may be carried out using the Legendre transform to compute the conjugate values of the mechanical and thermal momentum as

$$\mathbf{p}_a = \frac{\partial \mathbf{L}_h}{\partial \dot{\varphi}_a} = \sum_{b=1}^{n_d} m_{ab} \dot{\varphi}_b \quad \text{and} \quad \tau_a = \frac{\partial \mathbf{L}_h}{\partial \theta_a} = -\frac{\partial \mathbf{W}_h}{\partial \theta_a} = \Upsilon_a(\varphi_h, \Phi_h, \theta_h), \quad (30a)$$

respectively, for any node a , where again partial derivatives are computed keeping all other nodal values constant. In the following we will use

$$\mathbf{p} = \{\mathbf{p}_1, \dots, \mathbf{p}_N\} \quad \text{and} \quad \boldsymbol{\tau} = \{\tau_1, \dots, \tau_N\}. \quad (30b)$$

The function $\mathbf{p}_a(\cdot)$ is invertible, since the mass matrix is. If for each set of values of (φ_h, Φ_h) the discrete Lagrangian \mathbf{L}_h is a strictly convex function of θ_h , then the function $\Upsilon_a(\varphi_h, \Phi_h, \cdot)$ is invertible. This is guaranteed because we assumed that \mathbf{A} is a strictly convex function of θ , the same requirement needed for the definition of $\hat{\theta}$ in (3). Under these conditions, we denote this inverse with

$$\hat{\theta}_h(\mathbf{X}; \varphi_h, \Phi_h, \boldsymbol{\tau}) = \sum_{a=1}^d N_a(\mathbf{X}) \hat{\theta}_a(\varphi_h, \Phi_h, \boldsymbol{\tau}) \in V_h. \quad (30c)$$

where $\{\hat{\theta}_a\}_a$ are its nodal values. Notice that $\hat{\theta}_h$ is a different function than $\hat{\theta}$ in (3). Correspondingly, we define the discrete entropy density field as

$$\eta_h(\mathbf{X}; \varphi_h, \Phi_h, \boldsymbol{\tau}) = \eta(\nabla \varphi_h(\mathbf{X}), \hat{\theta}_h(\mathbf{X}; \varphi_h, \Phi_h, \boldsymbol{\tau})), \quad (30d)$$

where, although not essential, we have used the assumed independence of η on $\boldsymbol{\beta}$. The Hamiltonian for the semi-discrete system then follows as

$$\begin{aligned} H_h(\varphi_h, \Phi_h, \mathbf{p}, \boldsymbol{\tau}) &= \sum_{b=1}^N \left(\tau_b \hat{\theta}_b + \mathbf{p}_b \sum_{a=1}^N (m^{-1})_{ba} \mathbf{p}_a \right) - \mathbf{L}_h \\ &= \frac{1}{2} \sum_{a,b=1}^{n_d} \mathbf{p}_a \cdot (m^{-1})_{ab} \mathbf{p}_b + \rho_0 \sum_{p=1}^{N_q} w_p \mathbf{U}(\nabla \varphi_h(\boldsymbol{\xi}_p), \nabla \Phi_h(\boldsymbol{\xi}_p), \eta_h(\boldsymbol{\xi}_p; \varphi_h, \Phi_h, \boldsymbol{\tau})) + E_h(\varphi_h, \Phi_h). \end{aligned} \quad (30e)$$

where \mathbf{U} is the internal energy density per unit mass from (5).

3.2 Discretization in time: variational integrators

The final step consists in constructing approximations in time to the semi-discrete trajectories that solve (29). To this end, we partition the time interval $[0, T]$ with a time-step $\Delta t = T/M$,

$M > 1$, and set $t^k = kT/M$, $k = 0, \dots, M$. We denote by (φ_a^k, Φ_a^k) the approximation of $(\varphi_a(t^k), \Phi_a(t^k))$ computed by the algorithm, and use (24) to compute $(\varphi_h(\mathbf{X}, t^k), \Phi_h(\mathbf{X}, t^k))$ as the approximation to $(\varphi(\mathbf{X}, t^k), \Phi(\mathbf{X}, t^k))$ for all $\mathbf{X} \in K$, $\forall K \subset \mathcal{T}_h$.

The construction of variational integrators proceeds by defining approximations of the action obtained from (26). Since in this case the Lagrangian depends on the velocities in an other than quadratic way (specifically, the temperature), some care is needed to construct explicit second-order integrators in time. In the following we follow the ideas in [46]. We begin by defining the two discrete Lagrangians

$$\mathbf{L}_{h,\Delta t}^i(\varphi_h^0, \Phi_h^0, \varphi_h^1, \Phi_h^1) = \Delta t \mathbf{L}_h\left(\varphi_h^i, \Phi_h^i, \frac{\varphi_h^1 - \varphi_h^0}{\Delta t}, \frac{\Phi_h^1 - \Phi_h^0}{\Delta t}\right) \quad (31)$$

for $i = 0, 1$, and from here the class of discrete Lagrangians

$$\mathbf{L}_{h,\Delta t}^\alpha = (1 - \alpha)\mathbf{L}_{h,\Delta t}^0 + \alpha\mathbf{L}_{h,\Delta t}^1 \quad (32)$$

for any $\alpha \in [0, 1]$. For completeness, the expressions for the discrete Lagrangians in (31) are

$$\mathbf{L}_{h,\Delta t}^i = \Delta t \left(\sum_{a,b=1}^N \frac{m_{ab}}{2\Delta t^2} (\varphi_a^1 - \varphi_a^0) \cdot (\varphi_b^1 - \varphi_b^0) - \mathbf{W}_h\left(\varphi_h^i, \Phi_h^i, \frac{\Phi_h^1 - \Phi_h^0}{\Delta t}\right) - \mathbf{E}_h(\varphi_h^i, \Phi_h^i) \right) \quad (33)$$

for $i = 0, 1$. For each α , the algorithm follows by forming the discrete action sum

$$\mathbf{S}_d(\varphi_h^0, \Phi_h^0, \dots, \varphi_h^M, \Phi_h^M) = \sum_{k=0}^{M-1} \mathbf{L}_{h,\Delta t}^\alpha(\varphi_h^k, \Phi_h^k, \varphi_h^{k+1}, \Phi_h^{k+1}) \quad (34)$$

and finding $(\varphi_h^0, \Phi_h^0, \dots, \varphi_h^M, \Phi_h^M)$ satisfying the boundary conditions (27) at each time t^k , $k = 0, \dots, M$, that is a stationary point of \mathbf{S}_d among all admissible variations. These are the variations that keep (φ_h^0, Φ_h^0) and (φ_h^M, Φ_h^M) fixed and are zero on the Dirichlet boundary of each field (Γ_φ and Γ_Φ). This leads to the Discrete Euler-Lagrange equations, which in position-momentum form (see [69]) read

$$\begin{aligned} \mathbf{p}_a^k &= -D_{1a}\mathbf{L}_{h,\Delta t}^\alpha(\varphi_h^k, \Phi_h^k, \varphi_h^{k+1}, \Phi_h^{k+1}) = \sum_{b=1}^N m_{ab} \frac{(\varphi_b^{k+1} - \varphi_b^k)}{\Delta t} + (1 - \alpha)\Delta t (\mathbf{S}_a^{0,k} - \mathbf{B}_a^k) \quad (35a) \\ \mathbf{p}_a^{k+1} &= D_{3a}\mathbf{L}_{h,\Delta t}^\alpha(\varphi_h^k, \Phi_h^k, \varphi_h^{k+1}, \Phi_h^{k+1}) = \sum_{b=1}^N m_{ab} \frac{(\varphi_b^{k+1} - \varphi_b^k)}{\Delta t} - \alpha\Delta t (\mathbf{S}_a^{1,k} - \mathbf{B}_a^{k+1}) \quad (35b) \\ \tau_a^k &= -D_{2a}\mathbf{L}_{h,\Delta t}^\alpha(\varphi_h^k, \Phi_h^k, \varphi_h^{k+1}, \Phi_h^{k+1}) = (1 - \alpha)\Upsilon_a^{0,k} + \alpha\Upsilon_a^{1,k} - (1 - \alpha)\Delta t (\mathbf{H}_a^{0,k} + \mathbf{Q}_a^k) \quad (35c) \\ \tau_a^{k+1} &= D_{4a}\mathbf{L}_{h,\Delta t}^\alpha(\varphi_h^k, \Phi_h^k, \varphi_h^{k+1}, \Phi_h^{k+1}) = (1 - \alpha)\Upsilon_a^{0,k} + \alpha\Upsilon_a^{1,k} + \alpha\Delta t (\mathbf{H}_a^{1,k} + \mathbf{Q}_a^{k+1}) \quad (35d) \end{aligned}$$

for each nodal value admitting a variation, where $D_{ia}\mathbf{L}_{h,\Delta t}^\alpha$ denotes the partial derivative of $\mathbf{L}_{h,\Delta t}^\alpha$ with respect to the value at node a of its i -th argument, \mathbf{p}_a^k is numerical approximation to the nodal value of the mechanical momentum at t^k , and τ_a^k is the corresponding approximation to the thermal momentum. Additionally,

$$\begin{aligned} \mathbf{S}_a^{i,k} &= \mathbf{S}_a\left(\varphi_h^{k+i}, \Phi_h^{k+i}, \frac{\Phi_h^{k+1} - \Phi_h^k}{\Delta t}\right), & \mathbf{B}_a^k &= \mathbf{B}_a(\varphi_h^k, \Phi_h^k), & \mathbf{Q}_a^k &= \mathbf{Q}_a(\varphi_h^k, \Phi_h^k), \\ \Upsilon_a^{i,k} &= \Upsilon_a\left(\varphi_h^{k+i}, \Phi_h^{k+i}, \frac{\Phi_h^{k+1} - \Phi_h^k}{\Delta t}\right), & \mathbf{H}_a^{i,k} &= \mathbf{H}_a\left(\varphi_h^{k+i}, \Phi_h^{k+i}, \frac{\Phi_h^{k+1} - \Phi_h^k}{\Delta t}\right), \end{aligned} \quad (36)$$

for $i = 0, 1$. Explicit expressions for $\mathbf{S}_a^{i,k}$, $\Upsilon_a^{i,k}$, $\mathbf{H}_a^{i,k}$, \mathbf{B}_a^k , \mathbf{Q}_a^k are given in A.

Algorithm Equation (35) defines an algorithm, which given $(\varphi_h^k, \Phi_h^k, \mathbf{p}^k, \tau^k)$, returns $(\varphi_h^{k+1}, \Phi_h^{k+1}, \mathbf{p}^{k+1}, \tau^{k+1})$, for any $k \geq 0$. The basic procedure is as follows:

- (i) Solve (35a) and (35c) for $(\varphi_h^{k+1}, \Phi_h^{k+1})$.
- (ii) Update $(\mathbf{p}^{k+1}, \tau^{k+1})$ with (35b) and (35d), for $a = 1, \dots, N$.
- (iii) If of interest, an approximation of the temperature may be computed as

$$\theta_h^{k+1}(\mathbf{X}) = \hat{\theta}_h(\mathbf{X}; \varphi_h^{k+1}, \Phi_h^{k+1}, \tau^{k+1}), \quad (37)$$

and that of the velocity as

$$\dot{\varphi}_h^{k+1}(\mathbf{X}) = \sum_{a=1}^N \sum_{b=1}^N (m^{-1})_{ab} \mathbf{p}_b^{k+1} N_a(\mathbf{X}). \quad (38)$$

If a Gauss-Legendre (optimal) quadrature rule is used to evaluate the volume integrals, the resulting algorithm is implicit due to the coupling between different degrees of freedom introduced by the consistent mass matrix, by $H_a^{i,k}$, and by $\Upsilon_a^{i,k}$.

4 Explicit algorithms

In this section we derive two explicit schemes that exhibit second-order accuracy in both h and Δt by combining two ingredients: (i) a Gauss-Lobatto (GL) quadrature rule to compute the volume integrals appearing in (25a), (25b), and (25c), and (ii) a half-step composition of the methods obtained for $\mathbb{L}_{h,\Delta t}^0$ and $\mathbb{L}_{h,\Delta t}^1$.

The algorithms below are explicit in the sense that there is no coupled system of equations that needs to be solved. However, a nonlinear solver for a single scalar value could be needed at each node, depending on the constitutive relation.

4.1 Gauss-Lobatto quadrature rule

The GL rule adopts integration points at the nodes of the elements, which notably eliminates the coupling among different degrees of freedom. In particular, a lumped mass matrix is obtained. To compute the values of (36) under these conditions some care is needed, since ∇N_a is discontinuous at nodes. An explicit evaluation of the expressions given in A is not possible. Instead, the appropriate limit as the quadrature points approach each node from within each element is used. To make the resulting expressions explicit, it is convenient to define

$$w_{a,K} = \frac{1}{d+1} \text{Volume}(K) \quad (39)$$

for each node a and each element K in the ring of a , namely,

$$\text{ring}(a) = \{K \in \mathcal{T}_h \mid a \in K\}. \quad (40)$$

The weight of the quadrature point at a is then

$$w_a = \sum_{K \in \text{ring}(a)} w_{a,K}, \quad (41)$$

and the lumped mass matrix (29c) becomes $m_{ab} = \rho_0 \delta_{ab} w_a$ (no sum over a). With these definitions, and noticing that $\xi_a = \mathbf{X}_a$ and $N_a(\xi_b) = \delta_{ab}$, we get

$$\mathbf{S}_a^{i,k} = \mathbf{S}_a \left(\varphi_h^{k+i}, \Phi_h^{k+i}, \frac{\Phi_a^{k+1} - \Phi_a^k}{\Delta t} \right) = \sum_{\text{ring}(a)} w_{a,K} \mathbf{P} \left(\nabla \varphi_h^{k+i}|_K, \nabla \Phi_h^{k+i}|_K, \frac{\Phi_a^{k+1} - \Phi_a^k}{\Delta t} \right) \nabla N_a|_K \quad (42a)$$

$$\mathbf{B}_a^k = \mathbf{B}_a(\varphi_h^k) = -w_a \rho_0 \frac{\partial V_B}{\partial \varphi}(\varphi_a^k) + \sum_{j=1}^{N_t} w_j^t \mathbf{T} N_a(\xi_j^t) \quad (42b)$$

$$\mathbf{Q}_a^k = \mathbf{Q}_a = w_a \rho_0 \mathbf{Q} + \sum_{j=1}^{N_h} w_j^h (\bar{\mathbf{h}} N_a)(\xi_j^h), \quad (42c)$$

$$\Upsilon_a^{i,k} = \Upsilon_a \left(\varphi_h^{k+i}, \frac{\Phi_a^{k+1} - \Phi_a^k}{\Delta t} \right) = \sum_{\text{ring}(a)} \rho_0 w_{a,K} \eta \left(\nabla \varphi_h^{k+i}|_K, \frac{\Phi_a^{k+1} - \Phi_a^k}{\Delta t} \right), \quad (42d)$$

$$\mathbf{H}_a^{i,k} = \mathbf{H}_a(\varphi_h^{k+i}, \Phi_h^{k+i}) = \sum_{\text{ring}(a)} w_{a,K} \mathbf{h}(\nabla \varphi_h^{k+i}|_K, \nabla \Phi_h^{k+i}|_K) \nabla N_a|_K, \quad (42e)$$

where we have used the assumption that η does not depend on β and that \mathbf{h} does not depend on θ , as well as the form of \mathbf{E}_h , to only keep the arguments that the functions above depend on.

Finally, as mentioned earlier, the nodal values of the temperature θ_a^{k+1} needed for the temperature field θ_h^{k+1} in (37) follow from solving (30c) for each node a . With this choice of quadrature the equation to be solved for θ_a^{k+1} takes the form

$$\tau_a^{k+1} = \Upsilon_a(\varphi_h^{k+1}, \theta_a^{k+1}) = \rho_0 \sum_{\text{ring}(a)} w_{a,K} \eta(\nabla \varphi_h^{k+1}|_K, \theta_a^{k+1}). \quad (43)$$

For the two constitutive models in §2.4 explicit expressions for θ_a^{k+1} can be obtained, so no numerical solutions are needed.

4.2 First order with Δt

First, we consider the following numerical algorithms:

1. For $\mathbf{L}_{h,\Delta t}^0$ we obtain a method $F_{h,\Delta t}^0(\varphi_h^k, \Phi_h^k, \mathbf{p}^k, \boldsymbol{\tau}^k) = (\varphi_h^{k+1}, \Phi_h^{k+1}, \mathbf{p}^{k+1}, \boldsymbol{\tau}^{k+1})$ which consists of
 - (a) Computing Φ_a^{k+1} from (35c), (42c), (42d), and (42e). This step might require solving an equation similar to (43) for each node, depending on the constitutive relation.
 - (b) Computing φ_a^{k+1} from (35a), taking advantage of the lumped mass matrix, together with (42a) and (42b).
 - (c) Computing $(\mathbf{p}_a^{k+1}, \tau_a^{k+1})$ from (35b) and (35d), together with (42).

This algorithm can be identified with a version of the *symplectic-Euler-A* method [61, 62, 63, 69] formulated for the (non-separable) Hamiltonian appearing in the G-N-II theory.

2. For $\mathbf{L}_{h,\Delta t}^1$ we obtain a method $F_{h,\Delta t}^1(\varphi_h^k, \Phi_h^k, \mathbf{p}^k, \boldsymbol{\tau}^k) = (\varphi_h^{k+1}, \Phi_h^{k+1}, \mathbf{p}^{k+1}, \boldsymbol{\tau}^{k+1})$ which consists of

- (a) Computing φ_a^{k+1} from (35a), taking advantage of the lumped mass matrix.
- (b) Computing Φ_a^{k+1} from (35c) and (42d). This step might require solving an equation similar to (43) for each node, depending on the constitutive relation.
- (c) Computing $(\mathbf{p}_a^{k+1}, \tau_a^{k+1})$ from (35b) and (35d), together with (42).

In this case, this algorithm can be identified with the *symplectic-Euler-B* method [69, 61, 62, 63].

For the constitutive models in §2.4 it is possible to solve the equations in steps 1a and 2b explicitly. For more general models, the strict convexity of \mathbf{A} with respect to θ implies the convexity of W_h with respect to θ_h as well, and from there the solvability of the resulting equations.

4.3 Second order with Δt — Autonomous case

The methods in § 4.2 are explicit. However, they are only first-order accurate with Δt (see, e.g., [69, pp. 402], [46]). A second-order algorithm can be easily obtained by composing a first-order integrator with its adjoint to produce a self-adjoint method, see [62, Ch. 2]. Those methods are symmetric and therefore have an even-order of accuracy. When the Dirichlet boundary conditions are constant in time ($\dot{\varphi} = \dot{\Phi} = 0$), the resulting mechanical system is governed by an autonomous Lagrangian, and the adjoint method to $F_{h,\Delta t}^1$ is $F_{h,\Delta t}^{*1} = F_{h,\Delta t}^0$ [69, 46]. We took advantage of this fact to formulate second-order methods for discrete adiabatic thermoelastic systems in [46]. Based on those ideas, we formulate a second-order accurate method $\hat{F}_{h,\Delta t}^{10}$ as

$$\hat{F}_{h,\Delta t}^{10} = F_{h,\Delta t/2}^1 \circ F_{h,\Delta t/2}^{*1} = F_{h,\Delta t/2}^1 \circ F_{h,\Delta t/2}^0. \quad (44)$$

A straightforward computation shows that the above composition method corresponds to the variational integrator derived from the following discrete Lagrangian

$$\begin{aligned} \mathcal{L}_{h,\Delta t}^{01}(\varphi_h^0, \Phi_h^0, \varphi_h^1, \Phi_h^1) = & \quad (45) \\ & \text{ext}_{\substack{\varphi_a^{1/2} = \varphi(\mathbf{X}_a) \text{ if } \mathbf{X}_a \in \Gamma_\varphi \\ \Phi_a^{1/2} = \Phi(\mathbf{X}_a) \text{ if } \mathbf{X}_a \in \Gamma_\Phi}} \left[\mathcal{L}_{h,\Delta t/2}^0(\varphi_h^0, \Phi_h^0, \varphi_h^{1/2}, \Phi_h^{1/2}) + \mathcal{L}_{h,\Delta t/2}^1(\varphi_h^{1/2}, \Phi_h^{1/2}, \varphi_h^1, \Phi_h^1) \right], \end{aligned}$$

The resulting scheme is given in §4.5. A few remarks are appropriate:

- (i) Since the Hamiltonian of the system is non-separable, the obtained composition method does not coincide with Newmark's algorithm, as we noted earlier [63, 46].
- (ii) Another alternative to formulate an explicit, second-order variational time integrator is given by

$$\hat{F}_{h,\Delta t}^{01} = F_{h,\Delta t/2}^0 \circ F_{h,\Delta t/2}^1,$$

namely, by inverting the order of the composition in (44) or, equivalently, inverting the order of the discrete Lagrangians $\mathcal{L}_{h,\Delta t}^1$ and $\mathcal{L}_{h,\Delta t}^0$ in (45).

- (iii) Numerical algorithms in position-momentum form require the specification of initial conditions in terms of the nodal values $(\mathbf{p}_a(0), \tau_a(0))$. These can be computed with the help of (30a) from the initial configuration and the initial velocities and entropies $(\mathbf{v}_a^0, \theta_a^0)$. We do this in the algorithm in §4.5.

- (iv) A more compact algorithm could be possible by grouping some of the steps in the algorithm in §4.5, and a computer implementation could benefit from that. For the sake of clarity, in displaying the algorithm we kept precisely the steps involved from regarding the algorithm as the composition of the two first-order algorithms. We did obviate the computation of quantities in the midpoint of a step that were not needed later.

4.4 Second order with Δt — Non-autonomous case

The construction of second-order integrators in time when the functions $\overline{\varphi}(\mathbf{X}_a, t)$ and $\overline{\Phi}(\mathbf{X}_a, t)$ in (27) are other than constant needs some further care ². The essential reason behind it is that higher order methods require a higher-order sampling of these functions. It is not hard to see that in this case algorithms $F_{h,\Delta t/2}^0$ and $F_{h,\Delta t/2}^1$ cease to be adjoint to each other.

The effect of the time-dependent Dirichlet boundary conditions is to transform the mechanical system into one with a non-autonomous Lagrangian. To formulate higher-order variational integrators for this case, it is convenient to recover an autonomous Lagrangian by including time as one more generalized coordinate of the system, see [69, Part 4]. In this extended configuration manifold, an integration algorithm maps $(t^k, \varphi_h^k, \Phi_h^k, \mathbf{p}^k, \boldsymbol{\tau}^k)$ to $(t^k + \Delta t, \varphi_h^{k+1}, \Phi_h^{k+1}, \mathbf{p}^{k+1}, \boldsymbol{\tau}^{k+1})$. The key consequence of this perspective is that time is regarded as a variable that is equivalent to φ_h or Φ_h , so in the symplectic-Euler-A method Dirichlet boundary conditions are evaluated at the beginning of the time step, while this is done at the end of the time step in the symplectic-Euler-B method. Under these conditions, these two algorithms are again adjoint to each other, so their composition renders a second-order method, which is what is shown in the algorithm §4.5. For constant (or in this case also affine) Dirichlet boundary conditions in time, this algorithm coincides with that of §4.3, but they differ otherwise. The difference lies in that in this algorithm the values *and* the time derivatives of $\overline{\varphi}$ and $\overline{\Phi}$ are evaluated, while in the algorithm in §4.3 the time derivatives of $\overline{\varphi}$ and $\overline{\Phi}$ are approximated by a simple finite difference formula.

We shall not further expand the discussion on this aspect of the algorithms here, since it requires a discussion of non-autonomous systems and the introduction of further notation, and it is only marginally related to the main goal of the paper.

4.5 Explicit second-order algorithm $\hat{F}_{h,\Delta t}^{10}$

The precise description of the algorithm follows below.

-
- 1: Input: $(\varphi_h^0, \mathbf{v}_h^0, \Phi_h^0, \theta_h^0)$
 - 2: Output: $(\varphi_h^i, \mathbf{v}_h^i, \Phi_h^i, \theta_h^i)$ for $i = 1, \dots, M$
 - 3:
 - 4: {Initialization}
 - 5: $\mathbf{p}_a^0 \leftarrow m_{aa} \mathbf{v}_a^0$ for all nodes a
 - 6: $\tau_a^0 \leftarrow \Upsilon_a(\varphi_h^0, \theta_a^0)$ for all nodes a .
 - 7: $\Delta t_{\text{eff}} \leftarrow \Delta t/2$.
 - 8:
 - 9: {Advance in time}
 - 10: **for** $k = 0$ to $M - 1$ **do**
 - 11: {First half, $F_{h,\Delta t_{\text{eff}}}^0$ }
-

²To be precise, they could be affine in time, and the algorithm would still be second-order.

```

12: for all nodes  $a$  do
13:   if  $\mathbf{X}_a \in \Gamma_\Phi$  then
14:      $\theta_a^{\text{pre}} \leftarrow \bar{\Phi}(\mathbf{X}_a, t^k)$ 
15:   else
16:      $\Phi_a^{k+1/2} \leftarrow \text{Solve for } \Phi_a^{k+1/2} \text{ from } \tau_a^k = \Upsilon_a \left( \varphi_h^k, (\Phi_a^{k+1/2} - \Phi_a^k) / \Delta t_{\text{eff}} \right) - \Delta t_{\text{eff}} [H_a(\varphi_h^k, \Phi_h^k) + Q_a]$ 
17:      $\theta_a^{\text{pre}} \leftarrow (\Phi_a^{k+1/2} - \Phi_a^k) / \Delta t_{\text{eff}}$ 
18:      $\tau_a^{k+1/2} \leftarrow \Upsilon_a(\varphi_h^k, \theta_a^{\text{pre}})$ 
19:   end if
20:   if  $\mathbf{X}_a \notin \Gamma_\varphi$  then
21:      $\varphi_a^{k+1/2} \leftarrow \varphi_a^k + \Delta t_{\text{eff}} \mathbf{p}_a^k / m_{aa} - \Delta t_{\text{eff}}^2 [S_a(\varphi_h^k, \Phi_h^k, \theta_a^{\text{pre}}) - B_a(\varphi_h^k)] / m_{aa}$ 
22:      $\mathbf{p}_a^{k+1/2} \leftarrow m_{aa}(\varphi_a^{k+1/2} - \varphi_a^k) / \Delta t_{\text{eff}}$ 
23:   end if
24: end for
25:
26: {Second half,  $F_{h, \Delta t_{\text{eff}}}^1$ }
27: for all nodes  $a$  do
28:   if  $\mathbf{X}_a \in \Gamma_\varphi$  then
29:      $\varphi_a^{k+1} \leftarrow \bar{\varphi}(\mathbf{X}_a, t^{k+1})$ 
30:   else
31:      $\varphi_a^{k+1} \leftarrow \varphi_a^{k+1/2} + \Delta t_{\text{eff}} \mathbf{p}_a^{k+1/2} / m_{aa}$ 
32:   end if
33: end for
34: for all nodes  $a$  do
35:   if  $\mathbf{X}_a \in \Gamma_\Phi$  then
36:      $\Phi_a^{k+1} \leftarrow \bar{\Phi}(\mathbf{X}_a, t^{k+1})$ 
37:      $\theta_a^{\text{pre}} \leftarrow \dot{\bar{\Phi}}(\mathbf{X}_a, t^{k+1})$ 
38:   else
39:      $\Phi_a^{k+1} \leftarrow \text{Solve for } \Phi_a^{k+1} \text{ from } \tau_a^{k+1/2} = \Upsilon_a \left( \varphi_h^{k+1}, (\Phi_a^{k+1} - \Phi_a^{k+1/2}) / \Delta t_{\text{eff}} \right)$ 
40:      $\theta_a^{\text{pre}} \leftarrow (\Phi_a^{k+1} - \Phi_a^{k+1/2}) / \Delta t_{\text{eff}}$ 
41:   end if
42: end for
43: for all nodes  $a$  do
44:   if  $\mathbf{X}_a \in \Gamma_\varphi$  then
45:      $\mathbf{v}_a^{k+1} \leftarrow \bar{\varphi}(\mathbf{X}_a, t^{k+1})$ 
46:      $\mathbf{p}_a^{k+1} \leftarrow m_{aa} \mathbf{v}_a^{k+1}$ 
47:   else
48:      $\mathbf{p}_a^{k+1} \leftarrow \mathbf{p}_a^{k+1/2} - \Delta t_{\text{eff}} [S_a(\varphi_h^{k+1}, \Phi_h^{k+1}, \theta_a^{\text{pre}}) - B_a(\varphi_h^{k+1})]$ 
49:      $\mathbf{v}_a^{k+1} \leftarrow \mathbf{p}_a^{k+1} / m_{aa}$ 
50:   end if
51:   if  $\mathbf{X}_a \in \Gamma_\Phi$  then
52:      $\theta_a^{k+1} \leftarrow \theta_a^{\text{pre}}$ 
53:      $\tau_a^{k+1} \leftarrow \Upsilon_a(\varphi_h^{k+1}, \theta_a^{k+1})$ 
54:   else
55:      $\tau_a^{k+1} \leftarrow \Upsilon_a(\varphi_h^{k+1}, \theta_a^{\text{pre}}) + \Delta t_{\text{eff}} [H_a(\varphi_h^{k+1}, \Phi_h^{k+1}) + Q_a]$ 
56:      $\theta_a^{k+1} \leftarrow \text{Solve for } \theta_a^{k+1} \text{ from } \tau_a^{k+1} = \Upsilon_a(\varphi_h^{k+1}, \theta_a^{k+1})$ 
57:   end if
58: end for

```

4.6 A note on the use of a nodal quadrature

Explicit time integrators in solid dynamics require the use of a lumped mass matrix. These are generally obtained through the GL quadrature rule for the case of P_1 finite elements (see, e.g., [84]). The introduction of such quadrature does not deteriorate the spatial approximation properties of the scheme for linear elements [85, 86].

4.7 Conservation properties of the algorithms

As in §2.3, in this section we assume that $\Gamma_\varphi = \Gamma_\Phi = \emptyset$, for simplicity.

Momentum conservation One of the most attractive properties of VIs is that the discrete flows exactly conserve the quantities associated to symmetries of the discrete Lagrangians, due to a discrete analogue of Noether's theorem for continuous systems [64, 68, 83, 69]. We briefly review here the quantities conserved by this integrator, mostly focusing on the thermal parts, which have not been widely discussed.

The standard conserved mechanical quantities follow from the fact that the discrete Lagrangians proposed in (31) are invariant under the action of rigid body translations and rigid body rotations when, for example, $\mathbf{B} = 0$, $\mathbf{Q} = 0$, $\mathbf{T} = 0$, and $\bar{\mathbf{h}} = 0$, as the exact Lagrangian does, see §2.3. Therefore, the total linear momentum and the total angular momentum are automatically conserved by the algorithm. For completeness, the conserved quantities are computed as

$$\mathbf{L}_h^k = \sum_{a=1}^N \mathbf{p}_a^k \quad \text{and} \quad \mathbf{A}_h^k = \sum_{a=1}^N \boldsymbol{\varphi}_a^k \times \mathbf{p}_a^k, \quad (46)$$

for the linear and angular momenta, respectively.

If $\mathbf{Q} = 0$ and $\bar{\mathbf{h}} = 0$, the algorithm also conserves the total thermal momentum, namely, the value of the total entropy in the system as computed from the discretization:

$$\Xi_h^k = \sum_{a=1}^N \tau_a = \rho_0 \sum_{a=1}^N \sum_{\text{ring}(a)} w_{a,K} \eta(\nabla \boldsymbol{\varphi}_h^{k+1}|_K, \theta_a^{k+1}) \quad (47)$$

This follows from the symmetry of the discrete Lagrangian with respect to rigid translations of the thermal displacements. We briefly derive it next, essentially reproducing the steps of the discrete Noether's theorem shown in, for example, [64, 69]. To this end, consider a one parameter group of thermal displacements

$$\Phi_h^{k,\epsilon} = \Phi_h^k + \epsilon, \quad (48)$$

where $\epsilon \in \mathbb{R}$ is a constant. This corresponds to rigidly translating all thermal displacements by ϵ . A simple computation shows that the discrete Lagrangians (31) are invariant under the actions of this set of translations, i.e.,

$$\mathbb{L}_{h,\Delta t}^i(\boldsymbol{\varphi}_h^k, \Phi_h^{k,\epsilon}, \boldsymbol{\varphi}_h^{k+1}, \Phi_h^{k+1,\epsilon}) = \mathbb{L}_{h,\Delta t}^i(\boldsymbol{\varphi}_h^k, \Phi_h^k, \boldsymbol{\varphi}_h^{k+1}, \Phi_h^{k+1}),$$

for $i = 0, 1$, all $\epsilon \in \mathbb{R}$, and all $k = 0, \dots, M-1$, provided of course that $\mathbf{Q} = 0$ and $\bar{\mathbf{h}} = 0$. This property in turn implies the invariance of $\mathbf{L}_{h,\Delta t}^{01}$ and the invariance of its corresponding discrete action sum \mathbf{S}_d . Therefore,

$$\mathbf{L}_{h,\Delta t}^{01}(\varphi_h^k, \Phi_h^{k,\epsilon}, \varphi_h^{k+1}, \Phi_h^{k+1,\epsilon}) = \mathbf{L}_{h,\Delta t}^{01}(\varphi_h^k, \Phi_h^k, \varphi_h^{k+1}, \Phi_h^{k+1}). \quad (49)$$

It then follows that

$$0 = \frac{\partial \mathbf{S}_d}{\partial \epsilon} \Big|_{\epsilon=0} = \sum_{a=1}^N D_{2a} \mathbf{L}_{h,\Delta t}^{01}(\varphi_h^0, \Phi_h^0, \varphi_h^1, \Phi_h^1) + \sum_{a=1}^N D_{4a} \mathbf{L}_{h,\Delta t}^{01}(\varphi_h^{M-1}, \Phi_h^{M-1}, \varphi_h^M, \Phi_h^M), \quad (50)$$

over a discrete trajectory $(\varphi_h^0, \Phi_h^0, \dots, \varphi_h^M, \Phi_h^M)$, since by its definition $\partial \mathbf{S}_d / \partial \Phi_h^k = 0$ for $k = 1, \dots, M-1$. Using (35c) and (35d), we can rewrite this last equation as

$$\sum_{a=1}^N \tau_a^0 = \sum_{a=1}^N \tau_a^M. \quad (51)$$

The result in (47) then follows from (43), and from identifying M with any intermediate time step k .

Symplecticity of the discrete flow The exact flow of a Lagrangian system conserves a symplectic bilinear form, a straightforward consequence of its variational structure [69, 70, 87]. When discretized with a variational integrator, the same symplectic form is conserved by the discrete flow (see, e.g., [69, 64]). We do not reproduce the exact conserved form here, since it is a straightforward application of general results on variational integrators. In the context of continuum mechanics, a more general notion of symplecticity is also important, the so-called multi-symplecticity. For details, we refer the readers to [70, 68].

Energy conservation For an autonomous Lagrangian the total energy is exactly conserved along its trajectories. Unfortunately, symplectic numerical methods with constant time steps cannot be simultaneously symplectic and energy conserving [88, 67]. Despite the above limitation, symplectic integrators exhibit an excellent long term energy behavior when applied to Lagrangian systems. More specifically, Theorem 8.1 [62, Ch IX.8, pp.367] states that the energy of the numerical trajectories remains $\mathcal{O}(\Delta t^p)$ (p the order of the method) close to the exact one for exponentially long periods of time if a small enough time step is adopted. Therefore, the first law of thermodynamics is nearly exactly conserved by the discrete trajectories.

4.8 Stability

As an ad-hoc stability criterion for the explicit algorithms proposed here we have adopted that time steps are computed as a fraction of the Courant condition

$$\Delta t \leq \frac{h}{c_{\max}}, \quad (52)$$

where c_{\max} is the largest value of ω/K in (21), for a linear thermo-elastic material. We have verified numerically that this effectively behaves as the stability limit for this case.

5 Numerical examples

In this section we present numerical evidence of the properties of the algorithm $\hat{\mathbf{F}}_{h,\Delta t}^{10}$ from §4.5. The first example is devoted to show that the algorithm converges quadratically with both the mesh size and the time step. The second example is dedicated to show the conservation properties of the algorithm when simulating the dynamics of a nonlinear material.

5.1 Convergence Properties of the Algorithm

We begin by numerically observing the convergence rates of the algorithm. To this end, we constructed an exact solution that depends only on one of the spatial variables, so that we can simulate it and compare. Such solution was obtained in §2.4 for a linear and isotropic thermo-elastic material, by proposing harmonic solutions of the form $\boldsymbol{\varphi}(\mathbf{X}, t) = \mathbf{X} + u(X, t)\mathbf{e}_X$, with $u(X, t) = \Re[A_\varphi \exp[i(KX + \omega t)]]$, and $\Phi(\mathbf{X}, t) = \Re[A_\Phi \exp[i(KX + \omega t)]]$. Non-trivial solutions exist only if (21) holds. This implies that we require

$$A_\Phi = A_\varphi \frac{E/\rho_0 - (\omega/K)^2}{\gamma(\omega/K)}. \quad (53)$$

In one spatial dimensions over a finite interval $\Omega = (0, L)$, this is the solution of the initial value problem that satisfies (20) and the initial and boundary conditions

$$\begin{aligned} u(X, 0) &= \cos(KX), & \Phi(X, 0) &= \frac{E/\rho_0 - (\omega/K)^2}{\gamma(\omega/K)} \cos(KX), \\ \dot{u}(X, 0) &= -\omega \sin(KX), & \dot{\Phi}(X, 0) &= -\frac{E/\rho_0 - (\omega/K)^2}{\gamma(\omega/K)} \omega \sin(KX), \\ u(0, t) &= \cos(\omega t), & \Phi(0, t) &= \frac{E/\rho_0 - (\omega/K)^2}{\gamma(\omega/K)} \cos(\omega t), \\ u(L, t) &= \cos(KL + \omega t), & \Phi(L, t) &= \frac{E/\rho_0 - (\omega/K)^2}{\gamma(\omega/K)} \cos(KL + \omega t), \end{aligned} \quad (54)$$

for all $X \in (0, L)$ and all $t > 0$.

Out of the four possible values for ω in (21), we chose ω_{++} , so that ω is real. We set the material properties to $E = 20$, $\gamma = 0.1$, $c = 0.1$, $\rho_0 = 1$, $\kappa = 0.1$, $\theta_0 = 10$, and $\eta_0 = 0$, in standard SI units. Therefore, $c_{\max} = \omega_{++}/K = 4.67379$. For this example we set $\omega_{++} = 4$ and $A_\varphi = 1$, and computed $K = 0.855837$ and $A_\Phi = -3.94603$. The length of the domain is $L = 100$, and the domain was meshed with equal affine elements (two-node segments) with mesh sizes $h \in \{10, 5, 2.5, 1.25, 0.625, 0.3125, 0.15625\}$. The corresponding time steps were selected in order to respect (52), and were set to $\Delta t \in \{0.5, 0.25, 0.125, 0.0625, 0.03125, 0.15625, 0.078125\}$.

For a given time t^k , the error $e_{h,\Delta t}(t^k)$ associated with a particular mesh size and time step is computed as the relative L_2 -norm of the difference between some field $z_{h,\Delta t}^k(\mathbf{X})$ of the discrete solution and the corresponding field $z^*(\mathbf{X}, t^k)$ of the exact solution, namely

$$\begin{aligned} e_{h,\Delta t}(t^k) &= \frac{1}{z^*(t^k)} \sum_{e \in \mathcal{T}_h} \left(\sum_{p=1}^{N_q} w_p |z_{h,\Delta t}^k(\boldsymbol{\xi}_p) - z^*(\boldsymbol{\xi}_p, t^k)|^2 dV \right)^{\frac{1}{2}} \\ &\approx \frac{1}{z^*(t^k)} \left(\int_{\Omega} |z_{h,\Delta t}^k(\mathbf{X}) - z^*(\mathbf{X}, t^k)|^2 dV \right)^{\frac{1}{2}}, \end{aligned} \quad (55)$$

where $z^*(t) = (\int_{\Omega} z^*(\mathbf{X}, t)^2 dV)^{1/2}$, and $\{w_p, \xi_p\}_{p=1}^{N_q}$ is the Gauss-Legendre quadrature rule. Here z^* is one of the mechanical or thermal positions or velocities.

Figures 1 and 2 present the evolution of $e_{h,\Delta t}(1)$ with the pairs $(h, \Delta t)$. The algorithm exhibits a quadratic rate of convergence for both the error computed for the positions (φ, Φ) and the error computed for the velocities $(\dot{\varphi}, \theta)$. Figures 3 and 4 present snapshots of the exact and the numerical solutions for displacement and temperature at $t = 1$. In both cases, a zoomed out view of a smaller zone in the domain is also shown.

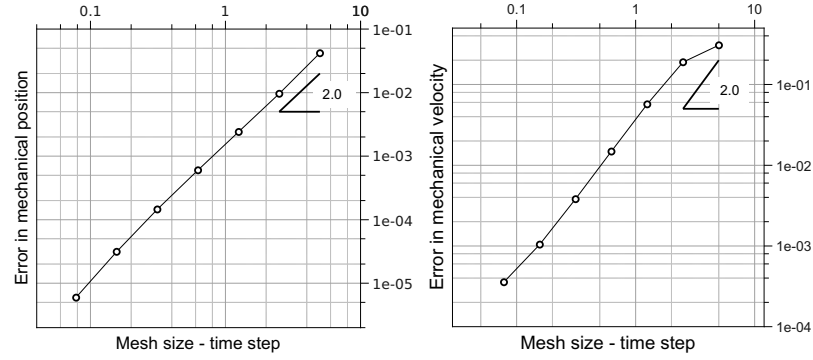


Figure 1: Convergence rate of the algorithm measured in terms of the L^2 -norm of the error in the mechanical (position and velocity) fields.

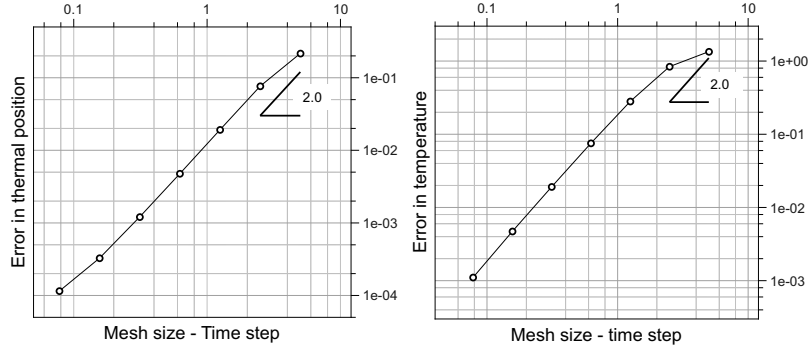


Figure 2: Convergence rate of the algorithm measured in terms of the L^2 -norm of the error in the thermal (position and velocity) fields.

5.2 Dynamics of a thermo-elastic three-dimensional body

In this example we simulate the dynamics of three-dimensional thermo-elastic beam that moves free of external mechanical or thermal forces. In this way, the energy, linear and angular momenta, and entropy of the beam have to be conserved through the motion. Thus, this example serves to illustrate the conservation properties of the algorithm.

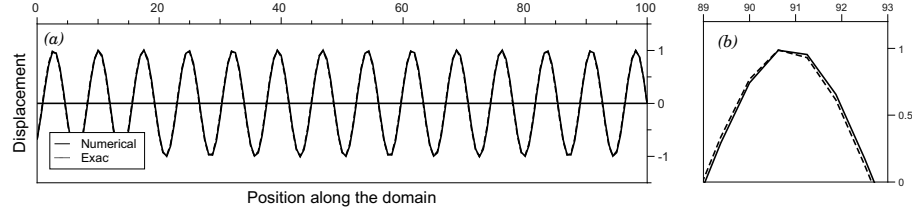


Figure 3: *a)* Exact and computed displacement field for one of the meshes we used. An enlarged view to observe the difference between the exact and the numerical solutions is also shown in *(b)*.

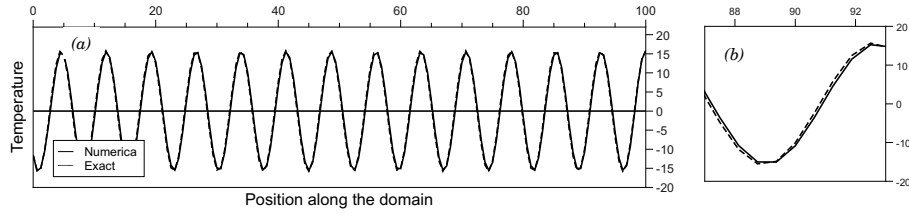


Figure 4: *a)* Exact and computed temperature field for one of the meshes we used. An enlarged view to observe the difference between the exact and the numerical solutions is also shown in *(b)*.

The geometric description of the beam is depicted in Fig. 5. It was discretized with 4608 affine tetrahedral elements, resulting in a total of 1061 nodes, see Fig. 6. The beam was assumed to be made of a material following the nonlinear constitutive relation (22), with $\rho_0 = 1.5$, $\mu = 83.33$, $\lambda = 55.55$, $\gamma = 0.5$, $\theta_0 = 10$, $c = 5$, $\eta_0 = 10$ and $\kappa = 1$, all of them in standard SI units.

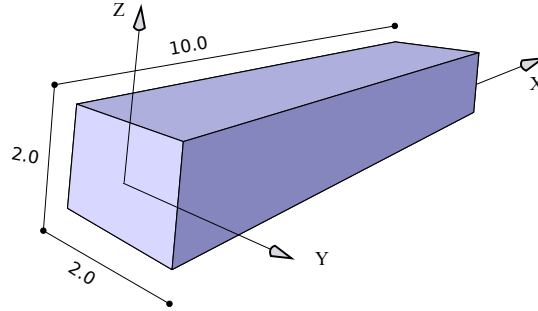


Figure 5: Three-dimensional view of the reference configuration for the thermo-elastic beam in this example.

To initiate the motion of the beam, we load it both mechanically and thermally for a short period of time, namely, 2.0 s. After that, the beam can move being traction-free and entropy-flux free on its entire boundary. Body forces and entropy sources per unit mass are absent as well throughout the simulation. The mechanical and thermal load during the first 2.0 s of the simulation is accomplished by setting

$$(i) \quad \Phi(\mathbf{X}, t) = \theta_0 t + \frac{40}{3} \sin\left(\frac{3}{10}t\right) \text{ if } \mathbf{X} \equiv (X, Y, Z) \in \{0\} \times [-1, 1] \times [-1, 1],$$

- (ii) $\varphi(\mathbf{X}, t) = (X - \frac{1}{4}t, Y - \frac{3}{2}t, Z + \frac{4}{5}t)$ if $\mathbf{X} \equiv (X, Y, Z) \in \{10\} \times [-1, 1] \times [-1, 1]$,
- (iii) Zero entropy flux wherever Φ is not specified, and
- (iv) Traction free wherever φ is not specified.

All constants above are, again, prescribed in appropriate SI unites. The time integration of this problem was performed with algorithm $\hat{\mathbf{F}}_{h,\Delta t}^{10}$ and a time step $\Delta t = 0.0025$ s.

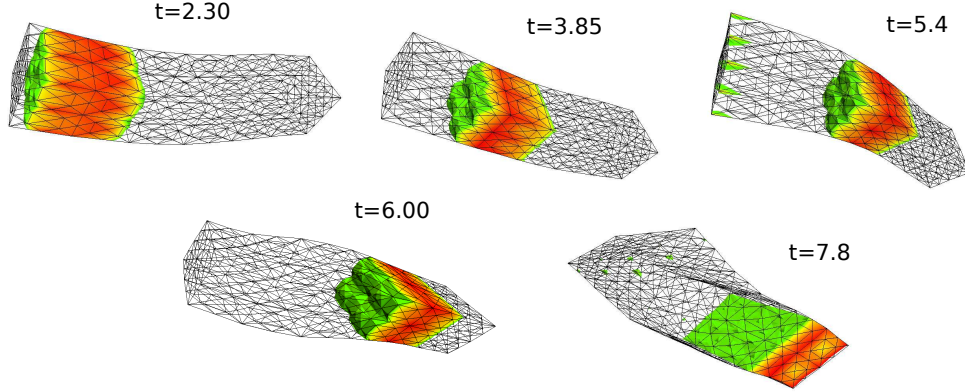


Figure 6: Sequence of snapshots during the free-fly phase of this numerical example, showing the deformed configuration of the beam and contours highlighting the parts of the beam with temperatures in the range $[10.5, 15]$.

The resulting dynamics of the beam is highly nonlinear involving forced vibrations due to the action of biaxial bending, twisting, shearing and compression that are simultaneously coupled with the nonlinear propagation of thermal waves. Fig. 6 shows a sequence of snapshots of the deformed shaped of the beam and volumetric contours highlighting the parts of the beam with temperatures in the range $[10.5, 15]$. As expected, the presence of thermal waves is clearly seen in the numerical solution.

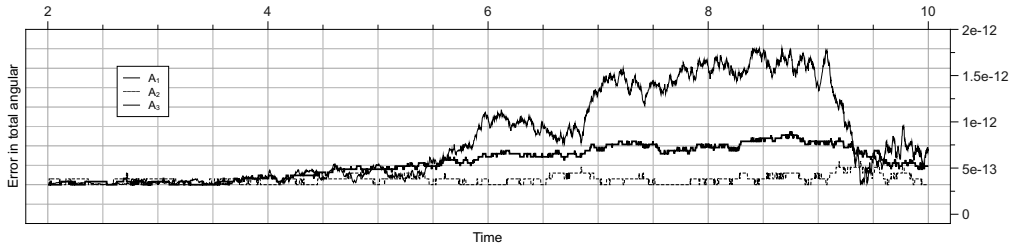


Figure 7: Error in the components of the total angular momentum \mathbf{A} .

The conservation properties of the proposed algorithm are verified in Figs. 7, 8 and 9, where it is seen that the total linear (\mathbf{L} , computed with (46)) and angular momentum (\mathbf{A} , computed with (46)), and the total entropy (Ξ , computed with (47) at each time step), are conserved up to round-off error after the external loading has ceased ($t > 2.0$ s). The specific

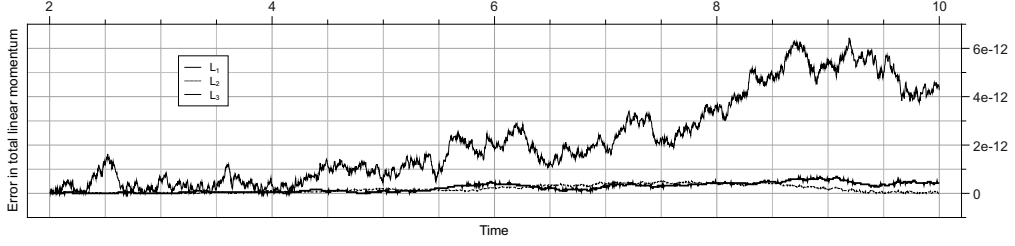


Figure 8: Error in the components of the total linear momentum \mathbf{L} .

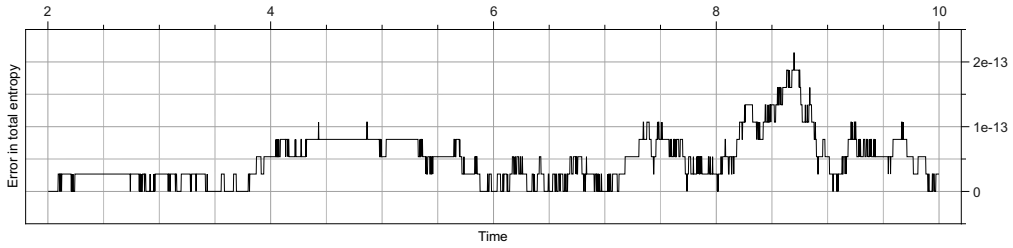


Figure 9: Error in the total entropy.

values that are conserved, as determined at $t = 2.0$ s, are

$$\begin{aligned}\mathbf{L} &= (31.85271482947, -351.2418171388, 187.4483240957) \\ \mathbf{A} &= (0.760167559539, -1337.826072699, -2508.077227983) \\ \Xi &= 3737.827302656\end{aligned}$$

where all the digits of the values that remain unchanged during the simulation are shown. The error in every component of those quantities in all the cases smaller than 10^{-11} .

The energy of the system H_h , from (30e), is not exactly conserved. However, as it is typical of variational or symplectic methods (see, e.g. [62]), it is nearly exactly conserved, with small oscillations around a value that is essentially conserved for exponentially long times as the time step decreases. This is what we observe in Fig. 10.

6 Conclusions

The Hamiltonian structure of Green and Naghdi theory of type II for thermo-elastic bodies with finite speed thermal waves enables the construction of variational integrators over finite element discretizations of the continuum problem. The resulting methods are said to be consistent with the laws of thermodynamics in the sense that, for adiabatic systems, (i) they nearly exactly conserve the total energy for an exponentially long period of time (first law), and (ii) they exactly conserve the total entropy of the system (second law). Moreover, they exactly conserve the total linear momentum and the total angular momentum of the system.

The challenge of formulating variational integrators that are thermodynamically consistent for bodies undergoing irreversible processes, such as heat conduction of Fourier type or inelastic constitutive relations, remains. Thermodynamic consistency in this case would amount to guaranteeing that for isolated systems the energy will be (nearly) conserved and that the entropy of the system will never decrease.

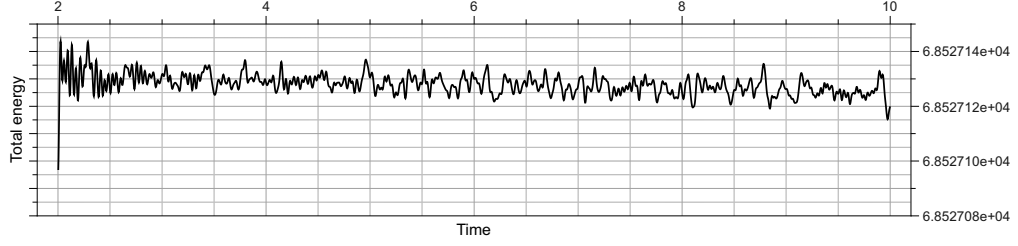


Figure 10: Time evolution of the total energy.

A Explicit expressions of derivatives of \mathbf{L}_h

The values of the derivatives of \mathbf{L}_h from §3.1 needed for the general algorithm in §3.2 are

$$\begin{aligned}
\mathbf{S}_a^{i,k} &= \frac{\partial \mathbf{W}_h}{\partial \varphi_a} \left(\varphi_h^{k+i}, \Phi_h^{k+i}, \frac{\Phi_h^{k+1} - \Phi_h^k}{\Delta t} \right) = \sum_{q=1}^{N_q} w_q \mathbf{P} \left(\nabla \varphi_h^{k+i}(\xi_q), \nabla \Phi_h^{k+i}(\xi_q), \frac{\Phi_h^{k+1} - \Phi_h^k}{\Delta t}(\xi_q) \right) \nabla N_a(\xi_q), \\
\mathbf{B}_a^k &= -\frac{\partial \mathbf{E}_h}{\partial \varphi_a}(\varphi_h^k, \Phi_h^k) = -\sum_{q=1}^{N_q} w_q \rho_0 \frac{\partial V_B}{\partial \varphi}(\varphi_h^k(\xi_q)) N_a(\xi_q) + \sum_{j=1}^{N_t} w_j^t \mathbf{T} N_a(\xi_j^t), \\
\mathbf{Q}_a^k &= -\frac{\partial \mathbf{E}_h}{\partial \Phi_a}(\varphi_h^k, \Phi_h^k) = \sum_{q=1}^{N_q} w_q \rho_0 \mathbf{Q} N_a(\xi_q) + \sum_{j=1}^{N_h} w_j^h (\bar{\mathbf{h}} N_a)(\xi_j^h), \\
\mathbf{T}_a^{i,k} &= -\frac{\partial \mathbf{W}_h}{\partial \theta_a} \left(\varphi_h^{k+i}, \Phi_h^{k+i}, \frac{\Phi_h^{k+1} - \Phi_h^k}{\Delta t} \right) = \rho_0 \sum_{q=1}^{N_q} w_q \eta \left(\nabla \varphi_h^{k+i}(\xi_q), \frac{\Phi_h^{k+1} - \Phi_h^k}{\Delta t}(\xi_q) \right) N_a(\xi_q), \\
\mathbf{H}_a^{i,k} &= -\frac{\partial \mathbf{W}_h}{\partial \Phi_a} \left(\varphi_h^{k+i}, \Phi_h^{k+i}, \frac{\Phi_h^{k+1} - \Phi_h^k}{\Delta t} \right) = \sum_{q=1}^{N_q} w_q \mathbf{h}(\nabla \varphi_h^{k+i}(\xi_q), \nabla \Phi_h^{k+i}(\xi_q)) \nabla N_a(\xi_q),
\end{aligned}$$

where we have used the assumption that η does not depend on β and that \mathbf{h} does not depend on θ .

References

- [1] Gurtin, M.E. and Pipkin, A.C. A general theory of heat conduction with finite wave speed. *Archive for Rational Mechanics and Analysis*. (1968) 31(2):113-126.
- [2] Malvern, L.E. *Introduction to the mechanics of a continuous medium*, Prentice Hall, 1997.
- [3] Marsden, J.E. and Hughes, T.J.R. *Mathematical Foundations of Elasticity*, Prentice-Hall, 1983.
- [4] Truesdell, C. and Noll, W. *Non-Linear Field Theories of Mechanics. Handbook of Physics, Vol. III/3*, Springer, Berlin, 1965.
- [5] Chandrasekharaiah, D.S. Hyperbolic thermoelasticity: A review of recent literature. *Applied Mechanics Reviews*. (1998) 51(12):705-729.

- [6] Dreyer, W. and Struchtrup, H. Heat pulse experiments revisited. *Continuum Mechanics and Thermodynamic*. (1993) 5:3-50.
- [7] Carey, G.F. and Tsai, M. Hyperbolic heat transfer with reflection. *Numerical Heat Transfer*. (1982) 5:309-327.
- [8] Shen, W. and Little, L. and Hu, L. Anti-diffusive methods for hyperbolic heat transfer. *Computer Methods in Applied Mechanics and Engineering*. (2010) 199:1231-1239.
- [9] Zhoua, J. and Zhanga, Y. and Chen, J.K. Non-Fourier Heat Conduction Effect on Laser-Induced Thermal Damage in Biological Tissues. *Numerical Heat Transfer, Part A: Applications*. (2008) 54(1):1-19.
- [10] Chester, M. Second sound in solids. *Physical Review*. (1963) 131(5) 2013-2015.
- [11] Lord, H.W. and Shulman, Y. A generalized dynamical theory of thermoelasticity. *Journal of the Mechanics and Physics of Solids*. (1967) 15:299-309.
- [12] Bogy, D.B. and Naghdi, P.M. On heat conduction and wave propagation in rigid solids. *Journal of Mathematical Physics*. (1970) 11(3):917-923.
- [13] Wall, D.J.N. and Olsson, P. Invariant imbedding and hyperbolic heat waves. *Journal of Mathematical Physics*. (1997) 38(3):1723-1749.
- [14] Ignaczak, J. and Ostoja-Starzewski, M. *Thermoelasticity with finite wave speeds*. Oxford Mathematical Monographs. Oxford University Press, 2010.
- [15] Vujanovic, B.D. and Baclic, B.S. Variational solutions of transient heat conduction through bodies of finite length. *Advances in Heat Transfer*. (1994) 24:39-99.
- [16] Vujanovic, B. and Strauss, A.M. Heat transfer with nonlinear boundary conditions via a variational principle. *American Institute of Aeronautics and Astronautics (AIAA-Journal)*. (1971) 9(2):327-330.
- [17] Vujanovic, B. A variational principle for non-conservative dynamical systems. *Journal of Applied Mathematics and Mechanics, ZAMM*. (1975) 55:321-331.
- [18] Vujanovic, B.D. and Jones, S.E. *Variational methods in nonconservative phenomena*, Academic Press, Inc. Mathematics in Science and Engineering, 1988.
- [19] Yang, Q. and Stainier, L. and Ortiz, M. A variational formulation of the coupled thermo-mechanical boundary-value problem for general dissipative solids. *Journal of the Mechanics and Physics of Solids*. (2006) 56:401-424.
- [20] Gambar, K. and Markus, F. Hamilton-Lagrange formalism of nonequilibrium thermodynamics. *Physical Review E*. (1994) 50(2):1227-1231.
- [21] Cannarozzi, A.A. and Ubertini, F. A mixed variational method for linear coupled thermoelastic analysis. *International Journal of Solids and Structures*. (2001) 38:717-739.
- [22] Sieniutycz, S. and Stephen, B.R. Least-entropy generation: Variational principle of Onsager's type for transient hyperbolic heat and mass transfer. *Physical Review A*. (1992) 46:6359-6370.

- [23] Mielke, A. and Ortiz, M. A class of minimum principles for characterizing the trajectories and the relaxation of dissipative systems. *ESAIM. Control, Optimization and Calculus of Variations*. (2008) 14:494-516.
- [24] Vujanovic, B. and Djukic, D.J. On the variational principle of Hamilton's type for nonlinear heat transfer problem. *International Journal of Heat Mass Transfer*. (1971) 15:1111-1123.
- [25] Green, A.E. and Naghdi, P.M. Thermoelasticity without energy dissipation. *Journal of elasticity*. (1993) 31(3):189-208.
- [26] Green, A. and Naghdi, P. A re-examination of the basic postulates of thermomechanics. *Proceedings: Mathematical and Physical Sciences*. (1991) 432:171-194.
- [27] Green, A. and Naghdi, P. A unified procedure for construction of theories of deformable media. I. Classical continuum physics. *Mathematical and Physical Sciences*. (1995) 448(1934):335-356.
- [28] Green, A. and Naghdi, P. On thermodynamics and the nature of the second law. *Proceedings of the Royal Society of London. Series A, Mathematical and Physical Sciences*. (1977) 357(1690):253-270.
- [29] Green, A.E. and Naghdi, P.M. On undamped heat waves in anelastic solid. *Journal of Thermal Stresses*. (1992) 15:253-264.
- [30] Maugin, G.A. Towards an analytical mechanics of dissipative materials. *Rendiconti del Seminario Matematico. Geometry, Continua and Microstructures. Universita e Politecnico di Torino, Torino*. (2000) 58(2):171-180.
- [31] Maugin, G.A. and Kalpakides, V.K. A Hamiltonian formulation for elasticity and thermoelasticity. *Journal of Physics A: Mathematical and General*. (2002) 35:10775-10788.
- [32] Dascalu, C. and Maugin, G.A. The Thermoelastic material-momentum Equation. *Journal of Elasticity*. (1995) 39:201-212.
- [33] Bargmann, S. and Steinmann, P. Classical results for a non-classical theory: remarks on thermodynamic relations in GreenNaghdi thermo-hyperelasticity. *Continuum Mechanics and Thermodynamics*. (2007) 19(1-2):59-66.
- [34] Bargmann, S. and Steinmann, P. Modeling and simulation of first and second sound in solids. *International Journal of Solids and Structures*. (2008) 45:6067-6073.
- [35] Quintanilla, R. Existence in thermoelasticity without energy dissipation. *Journal of Thermal Stresses*. (2002) 25:195-202.
- [36] Quintanilla, R. Thermoelasticity without energy dissipation of nonsimple materials. *Zeitschrift fr angewandte Mathematik und Mechanik*. (2003) 83(3):172-180.
- [37] Quintanilla, R. and Straughan, B. A note on discontinuity waves in type III thermoelasticity. *Proceedings of the Royal Society A*. (2004) 460:1169-1175.
- [38] Chandrasekharaiah, D.S. A Note on the uniqueness of solution in the linear theory of thermoelasticity without energy dissipation. *Journal of Elasticity*. (1996) 43:279-283.

- [39] Bargmann, S. and Steinmann, P. and Jordan, P.M. On the propagation of second-sound in linear and nonlinear media: Results from Green-Naghdi theory. *Physics Letters A*. (2008) 372:4418-4424.
- [40] Bargmann, S. and Denzer, R. and Steinmann, P. Material forces in non-classical thermo-hyperelasticity. *Journal of Thermal Stresses*. (2009) 32:361-393.
- [41] Armero, F. and Simo, J.C. A new unconditionally stable fractional step method for non-linear coupled thermomechanical problems. *International Journal for numerical methods in Engineering*. (1992) 35(4):737-766.
- [42] Farhat, C. and Park, K.C. and Dubois Pelerin, Y. An unconditionally stable staggered algorithm for transient finite element analysis of coupled thermoelastic problems. *Computer Methods in Applied Mechanics and Engineering*. (1991) 85:349-365.
- [43] Holzapfel, G.A. and Simo, J.C. A new viscoelastic constitutive model for continuous media at finite thermomechanical changes. *International Journal of Solids Structures*. (1996) 33:3019-3034.
- [44] Simo, J.C. and Miehe, C. Associative coupled thermoplasticity at finite strains: Formulation, numerical analysis and implementation. *Computer Methods in Applied Mechanics and Engineering*. (1992) 98(1):41-104.
- [45] Ibrahimbegovic, A. and Chorfi, L. and Gharzeddine, F. Thermomechanical coupling at finite elastic strain: covariant formulation and numerical implementation. *Communications in Numerical Methods in Engineering*. (2001) 17:275-289.
- [46] Mata, P. and Lew, A. Variational time integrators for finite dimensional thermoelasto dynamics without heat conduction. *International Journal for Numerical Methods in Engineering*. (2011) 88(1):1-30.
- [47] Romero, I. Thermodynamically consistent time-stepping algorithms for non-linear thermomechanical systems. *International Journal for Numerical Methods in Engineering*. (2009) 79:706-732.
- [48] Simo, J.C. and Wong, K.K. Unconditionally stable algorithms for rigid body dynamics that exactly preserve energy and momentum. *International Journal for Numerical Methods in Engineering*. (1991) 31(1):19-52.
- [49] Simo, J.C. and Tarnow, N. and Wong, K.K. Exact energy-momentum conserving algorithms and symplectic schemes for nonlinear dynamics. *Computer Methods in Applied Mechanics and Engineering*. (1992) 100:63-116.
- [50] Gonzalez, O. Exact energy and momentum conserving algorithms for general models in nonlinear elasticity. *Computer Methods in Applied Mechanics and Engineering*. (2000) 190:1763-1783.
- [51] Simo, J.C. and Tarnow, N. A new energy and momentum conserving algorithm for the non-linear dynamics of shells. *International Journal for Numerical Methods in Engineering*. (1994) 37(15):2527-2549.
- [52] Gross, M. and Betsch, P. An energy consistent hybrid space-time Galerkin method for nonlinear thermomechanical problems. *PAMM, Proceedings in Applied Mathematics and Mechanics*. (2006) 6:443-444.

- [53] Gross, M. and Betsch, P. On Deriving higher-order and energy-momentum-consistent time-stepping-schemes for thermo-viscoelastodynamics from a new hybrid space-time Galerkin method. *Proceedings of the ECCOMAS Thematic Conference on Multibody Dynamics*, 2007.
- [54] Krüger, M. and Groß, M. and Betsch, B. A comparison of structure-preserving integrators for discrete thermoelastic systems. *Computational Mechanics*. (2011) 47(6):701-722.
- [55] Hesch, C. and Betsch, P. Energy-momentum consistent algorithms for dynamic thermomechanical problems-Application to mortar domain decomposition problems. *International Journal for Numerical Methods in Engineering*. (2011) 86(11):1277-1378.
- [56] Romero, I. Algorithms for coupled problems that preserve symmetries and the laws of thermodynamics Part I: Monolithic integrators and their application to finite strain thermoelasticity. *Computer Methods in Applied Mechanics and Engineering*. (2010) 199:1841-1858.
- [57] Ottinger, H.C. *Beyond equilibrium thermodynamics*, John Wiley & Sons, Inc, 2005.
- [58] Bargmann, S. and Steinmann, P. Theoretical and computational aspects of non-classical thermoelasticity. *Computer Methods in Applied Mechanics and Engineering*. (2006) 196:516-527.
- [59] Bargmann, S. and Steinmann, P. Finite element approaches to non-classical heat conduction in solids. *Computer Modeling in Engineering & Science*. (2005) 9(2):133-150.
- [60] Bargmann, S. and Steinmann, P. An incremental variational formulation of dissipative and non-dissipative coupled thermoelasticity for solids. *Heat Mass Transfer*, (2008) 45:107-116.
- [61] Leimkuhler, B. and Reich, S. *Simulating Hamiltonian Dynamics*. *Cambridge Monographs on Applied and Computational Mathematics*, Cambridge University Press, 2004.
- [62] Hairer, E. and Lubich, C. and Wanner, G. *Geometric Numerical Integration. Structure-Preserving Algorithms for Ordinary Differential Equations*, Springer-Verlag, 2006.
- [63] Hairer, E. and Lubich, C. and Wanner, G. Geometric numerical integration illustrated by the Störmer-Verlet method. *Acta Numerica*. (2003) 12:399-450.
- [64] Lew, A. and Marsden, J.E. and Ortiz, M. and West, M. Variational time integrators. *International Journal for Numerical Methods in Engineering*. (2004) 60:153-212.
- [65] Veselov, A.P. Integrable discrete-time systems and difference operators. *Functional Analysis and Its Applications*. (1988) 22(2):83-93.
- [66] Moser, J. and Veselov, A.P. Discrete versions of some classical integrable systems and factorization of matrix polynomials. *Communications in Mathematical Physics*. (1991) 139(2):217-243.
- [67] Kane, C. and Marsden, J.E. and Ortiz, M. Symplectic-energy-momentum preserving variational integrators. *Journal of Mathematical Physics*. (1999) 40(7):3353-3371.
- [68] Lew, A. and Marsden, J.E. and Ortiz, M. and West, M. Asynchronous variational integrators. *Archive for Rational Mechanics and Analysis*. (2003) 2:85-146.

- [69] Marsden, J.E. and West, W. Discrete mechanics and variational integrators. *Acta Numerica*. (2001) 10:357-514.
- [70] Marsden, J.E. and Pekarsky, S. and Shkoller, S. and West, M. Variational methods, multisymplectic geometry and continuum mechanics. *Journal of Geometry and Physics*. (2001) 38:253-284.
- [71] Leyendecker, S. and Marsden, J.E. and Ortiz, M. Variational integrators for constrained dynamical systems. *ZAMM - Journal of Applied Mathematics and Mechanics / Zeitschrift für Angewandte Mathematik und Mechanik*. (2008) 88(9):677-708.
- [72] Fetecau, R.C. and Marsden, J.E. and Ortiz, M. and West, M. Nonsmooth Lagrangian mechanics and variational collision integrators. *SIAM Journal on Applied Dynamical Systems*. (2003) 2(3):381-416.
- [73] Cirak, F. and West, M. Decomposition contact response (DCR) for explicit finite element dynamics. *International Journal for Numerical Methods in Engineering*. (2005) 64:1078-1110.
- [74] Ryckman, R.A. and Lew, A.J. An explicit asynchronous contact algorithm for elastic body-rigid wall interaction. *International Journal for Numerical Methods in Engineering*. (2012) 89(7):869-896.
- [75] Harmon, D. and Vouga, E. and Smith, B. and Tamstorf, R. and Grinspun, E. Asynchronous contact mechanics. *ACM Transactions on Graphics (TOG) - Proceedings of ACM SIGGRAPH 2009 (Article 87)*. (2009) 28(3).
- [76] Stern, A. and Grinspun, E. Implicit-explicit variational integration of highly oscillatory problems. *Multiscale Modelling & Simulation*. (2009) 7(4):1779-1794.
- [77] Bou-Rabee, N. and Owhadi, H. Long-run accuracy of variational integrators in the stochastic context. *SIAM Journal on Numerical Analysis*. (2010) 48 (1):278-297.
- [78] Bou-Rabee, N. and Owhadi, H. Stochastic variational integrators. *IMA Journal of Numerical Analysis*. (2009) 29(2):421-443.
- [79] Lee, T. and Leok, M. and McClamroch, N.H. Lie group variational integrators for the full body problem. *Computer Methods in Applied Mechanics and Engineering*. (2007) 196(29-30):2907-2924.
- [80] Lee, T. and Leok, M. and McClamroch, N.H. Lagrangian mechanics and variational integrators on two-spheres. *International Journal for Numerical Methods in Engineering*. (2009) 79(9):1147-1174.
- [81] Gawlik, E.S. and Mullen, P. and Pavlov, D. and Marsden, J.E. and Desbrun, M. Geometric, variational discretization of continuum theories. *Physica D: Nonlinear Phenomena*. (2011) 240(21):1724-1760.
- [82] Maugin, G.A. and Kalpakides, V.K. The slow march towards an analytical mechanics of dissipative materials. *Technische Mechanik*. (2002) 22(2):98-103.
- [83] Lew, A. *Variational time integrators in computational solid mechanics*. California Institute of Technology, Pasadena, California, USA, 2003.

- [84] Hughes, T.J.R. *The Finite Element Method. Linear Static and Dynamic Finite Element Analysis*. Prentice-Hall Inc, 1987.
- [85] Cohen, G. and Joly, P. and Roberts, J.E. and Tordjman, N. Higher Order Triangular Finite Elements with Mass Lumping for the Wave Equation. *SIAM Journal on Numerical Analysis*. (2001) 38(6):2047-2078.
- [86] Durufle, M. and Grob, P. and Joly, P. Influence of Gauss and Gauss-Lobatto quadrature rules on the accuracy of a quadrilateral finite element method in the time domain. *Numerical Methods for Partial Differential Equations*. (2009) 25(3):526-551.
- [87] Marsden, J.E. and Ratiu, T.S. *Introduction to Mechanics and Symmetry*. Springer-Verlag, 1999.
- [88] Ge, Z. and Marsden, JE. Lie-Poisson Hamilton-Jacobi theory and Lie-Poisson integrators. *Physics Letters A*. (1988) 133(3):134-139.

